

https://doi.org/10.3799/dqkx.2018.711



拉萨地体北部永珠地区早白垩世岩浆岩地球化学、锆石 U-Pb 年代学、Hf 同位素组成及其地质意义

张诗启, 戚学祥, 韦 诚, 陈松永

中国地质科学院地质研究所, 北京 100037

摘要: 拉萨地体北部出露大面积早白垩世岩浆岩, 对它们的成因和形成机制的研究, 有助于揭示拉萨地块白垩纪时期的岩浆作用过程及动力学背景。通过岩石学、地球化学和同位素地质学方法对拉萨地体北带永珠地区早白垩世中—酸性岩浆岩进行了研究。结果显示黑云母二长花岗岩、流纹岩和安山岩的锆石 LA-ICP-MS U-Pb 年龄分别为 118 ± 1.0 Ma、 121 ± 0.8 Ma 和 115 ± 0.8 Ma, 代表了其侵入和喷出时代。黑云母二长花岗岩、花岗斑岩和流纹岩为高钾钙碱性过铝质—强过铝质岩浆岩 ($A/CNK=1.01 \sim 1.35$), 亏损高场强元素 Nb、P、Ti 和大离子亲石元素 Ba、Sr, 富集大离子亲石元素 Rb、K 和放射性元素 U、Th; 稀土配分图显示 LREE 富集, HREE 近平坦, Eu 明显负异常, 为形成于大陆边缘的岛弧岩浆岩特征。黑云母二长花岗岩和流纹岩的锆石 Hf 初始比值 $\epsilon_{\text{Hf}}(t)$ 分别为 $-1.21 \sim 3.01$ 和 $-0.68 \sim 5.35$, 对应的两阶段模式年龄分别为 $0.99 \sim 1.26$ Ga 和 $0.84 \sim 1.22$ Ga, 为壳幔混源岩浆。安山岩为高钾钙碱性, 亏损 Nb、Ta、P、Ti、U 和 Sr, 富集 Rb、K 和 Th, 稀土配分图显示 LREE 富集, HREE 近平坦, Eu 轻微负异常, 为形成于大陆边缘弧的岩浆岩。结合前人研究成果, 分析认为永珠地区早白垩世岩浆岩形成于班公湖—怒江特提斯洋壳南向俯冲作用下的大陆边缘弧环境, 由俯冲的班公湖—怒江中特提斯洋板片在深部脱水熔融, 进而诱发上覆地幔楔部分熔融形成基性岩浆上涌, 导致下地壳物质发生部分熔融形成酸性岩浆, 它们在上升过程中按不同比例混合, 形成中性和酸性岩浆侵入到地下或喷出地表, 形成侵入岩和火山岩。

关键词: 早白垩世岩浆岩; 地球化学; 锆石 U-Pb 年龄; 永珠地区。

中图分类号: P588.121; P597.3

文章编号: 1000-2383(2018)04-1085-25

收稿日期: 2017-12-18

Geochemistry, Zircon U-Pb Dating and Hf Isotope Compositions of Early Cretaceous Magmatic Rocks in Yongzhu Area, Northern Lhasa Terrane, Tibet, and Its Geological Significance

Zhang Shiqi, Qi Xuexiang, Wei Cheng, Chen Songyong

Institute of Geology, Chinese Academy of Geological Sciences, Beijing 100037, China

Abstract: The study on the petrogenesis and tectonic setting of the Early Cretaceous magmatic rocks in the northern Lhasa is important to define the geodynamic evolution for the Lhasa terrane. In this paper, it is reported of petrology, petrogeochemistry, zircon U-Pb ages and zircon Hf isotopic compositions of Early Cretaceous magmatic rocks from Yongzhu area in the northern Lhasa terrane. Zircon U-Pb ages for biotite-monzonitic granite, rhyolite and andesite are 118 ± 1.0 Ma, 121 ± 0.8 Ma and 115 ± 0.8 Ma respectively, representing their intrusion and eruption period. Biotite-monzonitic granite, granite porphyry and rhyolite show similar geochemical characteristics. They are high K calc-alkaline and weakly peraluminous-strongly peraluminous granites ($A/CNK=1.01-1.35$). In primitive mantle-normalized spider diagrams, these rocks are characterized by

基金项目: 国家自然科学基金项目 (Nos.91755101, 41272219); 中国地质调查局项目 (No.1212011020000150005-07); 科技部深部探测技术与实验研究专项 (No.SinoProbe-05-03)。

作者简介: 张诗启 (1982—), 男, 博士研究生, 主要从事构造地质学、岩石学专业研究。ORCID: 0000-0002-2394-6988. E-mail: zhangshiqi0396@163.com

引用格式: 张诗启, 戚学祥, 韦诚, 等. 2018. 拉萨地体北部永珠地区早白垩世岩浆岩地球化学、锆石 U-Pb 年代学、Hf 同位素组成及其地质意义. 地球科学, 43(4): 1085-1109.

enriched large ion lithophile elements Rb, K and radioactive elements U, Th, and negative anomalies in Nb, P, Ti, Ba and Sr. Chondrite-normalized REE patterns show that these rocks are enriched in LREE, nearly flat HREE and negative Eu anomalies. Above chemical natures suggest that they are island-arc igneous rocks and formed in continental margin arc setting. The Hf isotopic compositions in the biotite-monzonitic granite and rhyolite are -1.21 to 3.01 and -0.68 to 5.35 , respectively, and two stage model ages are $0.99-1.26$ Ga and $0.84-1.22$ Ga, respectively, which suggests mixed source of crust and mantle. In contrast, the andesite shows slightly different geochemical characteristics. They are characterized by (1) high K calc-alkaline; (2) negative anomalies in Nb, Ta, P, Ti, U and Sr, and enrichment of Rb, K and Th in primitive mantle-normalized spider diagrams; (3) chondrite-normalized REE patterns show that these rocks are enriched in LREE, nearly flat HREE, and slight negative Eu anomalies; (4) formation in the continental margin arc setting. It is proposed that the Early Cretaceous magmatic rocks in Yongzhu were formed in the continental margin arc setting. During southern subduction of Bangonghu-Nujiang Tethyan oceanic basin, dehydration melting of the subduction oceanic plate produced the high thermal molten mass, which induced partial melting of the mantle wedge and formation of mafic magma. Then upwelling of mafic magma induced partial melting of the lower crust material and formation of acidic magma. During ascent process of the mafic magma and acidic magma, the two types of magma mixed in different proportion, and formed volcanic and plutonic rocks.

Key words: Early Cretaceous magmatic rock; geochemistry; zircon U-Pb age; Yongzhu area.

0 引言

青藏高原中部班公湖—怒江中特提斯洋缝合带 (Yin and Harrison, 2000; Pan *et al.*, 2012; Metcalfe, 2013; Zhu *et al.*, 2016) 南缘, 自昂龙错至班戈县, 在东西长约 720 km、南北宽 20~40 km 范围内出露大面积岩浆岩, 构成了拉萨地体北部的昂龙岗日—班戈岩浆岩带 (潘桂棠等, 2006; 朱弟成等, 2006a, 2008; Zhu *et al.*, 2009, 2011; 耿全如等, 2011, 2015)。该带由形成于晚侏罗世—早白垩纪世 (137~110 Ma) 班公湖—怒江洋俯冲背景的岩浆岩 (朱弟成等, 2006a, 2008; Zhu *et al.*, 2009, 2011, 2016; 康志强等, 2009; 高顺宝等, 2011a; 黄瀚霄等, 2012; 孙赛军等, 2015) 和晚白垩世 (91~76 Ma) 后碰撞造山环境的岩浆岩 (Zhu *et al.*, 2011, 2013; 王江朋等, 2012; Wang *et al.*, 2014; 张志等, 2017) 组成。其中, 早白垩世岩浆岩的锆石 $\epsilon_{\text{Hf}}(t)$ 值为 $-30.4 \sim 18.8$ 之间, 它们的岩浆源区既有下地壳部分熔融 (Zhu *et al.*, 2011, 2013; 黄玉等, 2012; 孙赛军等, 2015), 又有壳幔物质混源 (张亮亮等, 2010; Zhu *et al.*, 2013; Wang *et al.*, 2014), 并且具有自北缘向南岩浆岩 $\epsilon_{\text{Hf}}(t)$ 值逐渐减小的特点, 指示班公湖—怒江洋壳南向俯冲的极性 (Zhu *et al.*, 2011, 2016)。关于拉萨地体北部早白垩世岩浆岩的成岩构造环境, 早期研究由于未发现拉萨地体南部存在早白垩世岩浆岩和认为晚侏罗世—早白垩世时拉萨地体与羌塘地体已碰撞 (Metcalfe, 1998; Yin and Harrison, 2000), 由此认为拉萨地体北部的早白垩世岩浆岩形成于拉萨—羌塘地体碰撞地壳增厚重熔

构造背景 (Xu *et al.*, 1985; Pearce and Mei, 1988; Harris and Massey, 1994); 随着在拉萨地体的南部和北部相继发现了早白垩世岩浆岩, 且早白垩世时期雅鲁藏布江新特提斯洋壳已开始北向俯冲 (Sengör *et al.*, 1988; Niu *et al.*, 2003; Yang *et al.*, 2011), 又有部分学者认为拉萨地体北部白垩纪岩浆活动是由雅鲁藏布江新特提斯洋壳向北俯冲所引起 (Coulon *et al.*, 1986; Copeland *et al.*, 1995; Ding *et al.*, 2003; Zhang *et al.*, 2004; Chu *et al.*, 2006; Decelles *et al.*, 2007; Kapp *et al.*, 2007; Chiu *et al.*, 2009); 近年来, 随着地质资料积累和研究的深入, 越来越多的研究者趋向于认为班公湖—怒江中特提斯洋壳在早白垩世持续南向俯冲于拉萨地体之下 (潘桂棠等, 2006; 朱弟成等, 2006a, 2008; 张亮亮等, 2010; 高顺宝等, 2011a), 并在约 110 Ma 发生断离来解释拉萨地体北部早白垩世的大规模岩浆活动 (Zhu *et al.*, 2011, 2016; 曲晓明等, 2012; 康磊等, 2012; Chen *et al.*, 2014)。因此, 拉萨地体北部早白垩世岩浆岩的成因和成岩构造环境有待进一步探讨。而且, 如此大规模的早白垩世岩浆岩, 目前仅盐湖花岗岩体、班戈花岗岩体和那曲地区的部分花岗岩体进行了 Lu-Hf 同位素精确示踪研究, 也一定程度制约了对早白垩世花岗岩的成因认识。同时, 拉萨地体北部永珠地区白垩纪岩浆岩以往仅对雄梅西 3 个面积均小于 1 km^2 的侵入岩体 (曲晓明等, 2012) 和多尼组火山岩 (康志强等, 2009) 开展了年代学和地球化学初步研究, 研究表明它们均成岩于早白垩世 (110~116 Ma), 但成岩构造环境和成因尚存在洋壳俯冲、陆内伸展和幔源物质上涌、壳源物质重熔

的争议,因此,进一步对拉萨地体北部永珠地区早白垩世岩浆岩进行研究,不仅能加深对其成因的理解和成岩构造动力学背景的认识,还可对班公湖—怒江洋壳的俯冲时代和极性加以约束,有助于进一步认识青藏高原大地构造演化。

本文以班公湖—怒江缝合带中部永珠地区早白垩世岩浆岩为研究对象,开展了岩石学、岩石地球化学、锆石 U-Pb 年代学和 Lu-Hf 同位素研究,进而探讨它们的岩石成因和成岩构造动力学背景,以期对班公湖—怒江中特提斯洋的中生代演化提供一定程度的约束。

1 地质背景

青藏高原是由多个地体经历多期造山作用拼贴在一起的“造山的高原”(许志琴,2007; Yin and

Harrison,2000;许志琴等,2011),从北至南依次以金沙江、龙木措—双湖、班公湖—怒江和雅鲁藏布江缝合带为界,划分为松潘—甘孜、北羌塘、南羌塘、拉萨和喜马拉雅地块(图 1a)(潘桂棠等,2006;李才等,2009;Zhai *et al.*, 2011;Metcalf,2013;Zhu *et al.*, 2013),其中拉萨地块又以狮泉河—永珠—纳木措蛇绿混杂岩带(SNMZ)和洛巴堆—米拉山断裂(LMF)为界划分为北拉萨、中拉萨和南拉萨地体(图 1b),且出露大量晚侏罗世—白垩纪岩浆岩(朱弟成等,2008;Zhu *et al.*, 2011, 2013)。

伴随特提斯洋的形成和消亡,拉萨地体经历了复杂的演化过程,晚二叠世—晚三叠世期间拉萨地体自澳大利亚地块裂离并开始向北漂移(Sengör *et al.*, 1988;Yang *et al.*, 2009;Dong *et al.*, 2010;Zhu *et al.*, 2011, 2013;Metcalf,2013),晚侏罗世—早白垩世班公湖—怒江中特提斯洋壳向南俯冲

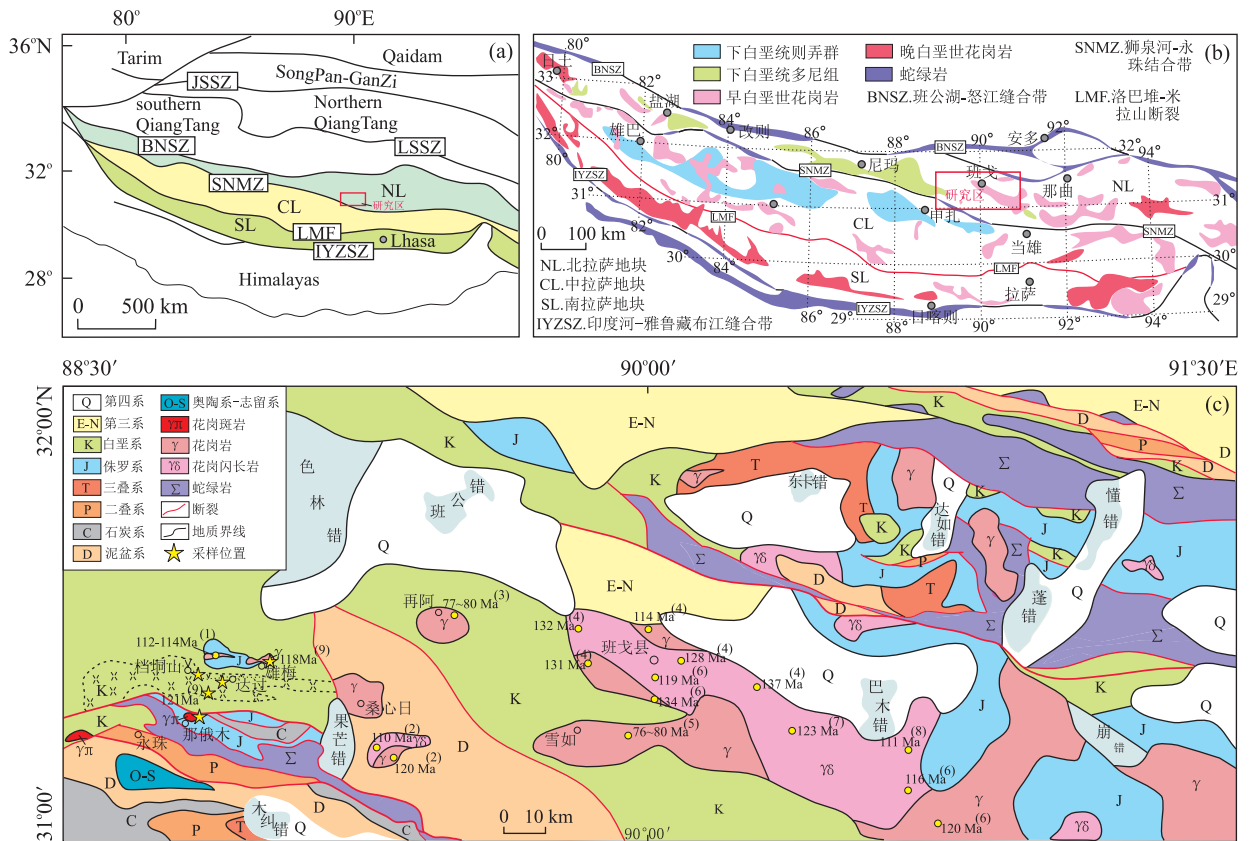


图 1 青藏高原大地构造简图(a)、拉萨地体白垩世岩浆岩分布图(b)和研究区区域地质简图(c)

Fig.1 Tectonic framework for the Tibetan Plateau (a), the Cretaceous igneous rocks of the Lhasa terrane (b), and the regional geological map of survey region (c)

图 a 据 Zhu *et al.*, 2013;图 b 据 Zhu *et al.*, 2011;图 c 据曲永贵等,2003;1:25 万多巴区幅区域地质图;陈玉禄等,2002;1:25 万班戈县幅区域地质图。图 a:JSSZ.金沙江缝合带;BNSZ.班公湖—怒江缝合带;SNMZ.狮泉河—纳木措混杂岩带;LMF.洛巴堆—米拉山断裂;IYZSZ.印度河—雅鲁藏布江缝合带;NL.北拉萨地体;CL.中拉萨地体;SL.南拉萨地体;LSSZ.龙木措—双湖缝合带;图 c 年龄数据来源:(1)曲晓明等,2012;(2)张乐,2015;(3)定立等,2012;(4)高顺宝等,2011a, 2011b;(5)王江朋等,2012;(6)Zhu *et al.*, 2016;(7)黄瀚霄等,2012;(8)Zhu *et al.*, 2011;(9)本文

于拉萨地体之下(Kapp *et al.*, 2003;莫宣学和潘桂棠, 2006;史仁灯, 2007; Zhu *et al.*, 2011, 2013; Li *et al.*, 2013a, 2014a; Hao *et al.*, 2016; Wang *et al.*, 2016), 早白垩世晚期(118~110 Ma)拉萨地体与南羌塘地体局部开始碰撞(Kapp *et al.*, 2007; Zhu *et al.*, 2011); 同时, 雅鲁藏布江新特提斯洋壳初始向拉萨地体之下俯冲(Sengör *et al.*, 1988; Niu *et al.*, 2003; Yang *et al.*, 2011), 早白垩世晚期—晚白垩世早期(± 110 Ma)拉萨地体和羌塘地体碰撞拼合(Zhu *et al.*, 2011, 2016; Fan *et al.*, 2014; Wang *et al.*, 2016), 新生代时期(65~34 Ma)印度大陆和欧亚大陆发生碰撞(Searle *et al.*, 1987; Yin and Harrison, 2000; 莫宣学等, 2003; Aitchison *et al.*, 2007; Mo *et al.*, 2007, 2008; Yin, 2010; Najman *et al.*, 2010; Chu *et al.*, 2011)的演化过程。伴随着拉萨地体的北移、特提斯洋壳的俯冲消减、以及拉萨地体与南羌塘和印度地块的碰撞, 拉萨地体内部形成了多期大规模的构造岩浆活动, 最终形成了拉萨地块现今的地质构造面貌。

拉萨地体北带由古生代—中生代海相碎屑岩和新生代陆相碎屑岩所覆盖, 局部出露少量新元古代念青唐古拉群变质岩(潘桂棠等, 2004; 莫宣学等, 2005; 朱弟成等, 2008; 耿全如等, 2011), 中生代岩浆岩大面积分布(137~76 Ma, 张亮亮等, 2010; Zhu *et al.*, 2011, 2016; 高顺宝等, 2011a; 曲晓明等, 2012; 王江朋等, 2012; 康磊等, 2012; 黄玉等, 2012; Chen *et al.*, 2014; 孙赛军等, 2015)。研究区位于拉萨地体北部的永珠—班戈县地区(图 1b), 出露古生代奥陶纪—二叠纪深—浅海相灰岩和碎屑岩, 中生代三叠纪海陆交互相碎屑岩夹灰岩, 侏罗纪滨—浅海相灰岩, 白垩纪滨—浅海相灰岩、长石石英砂岩、粉砂岩和流纹岩, 以及永珠蛇绿混杂岩(图 1c); 岩浆岩沿北西向主构造线展布, 岩石类型有花岗闪长岩、花岗岩、流纹岩、安山岩和少量玄武岩。

2 岩石学特征

为了全面揭示永珠地区早白垩世岩浆岩的形成时代和构造背景, 本文选择雄梅黑云母二长花岗岩、那俄木花岗斑岩和下白垩统多尼组火山岩进行岩石学、地球化学和同位素地质学研究。

雄梅黑云母二长花岗岩体(图 2, 图 3a, 3b): 位于雄梅区北侧, 近东西向展布, 长约 12 km, 宽 2~5 km, 出露面积约 50 km², 侵位于晚侏罗世灰岩中, 与灰岩接触部发育宽 3~5 m 的矽卡岩化带。岩石呈浅灰色, 块状构造, 中粒结构, 主要矿物为斜长石、钾长石、石英和黑云母。其中, 斜长石呈半自形—他形板柱状、粒度在(0.05 mm×0.25 mm)~(2 mm×3 mm)之间, 个别斜长石内存在微裂隙, 局部沿微裂隙有轻微绢云母化, 含量约 30%; 钾长石呈半自形—他形板状, 粒度一般在(0.1 mm×0.2 mm)~(1 mm×3 mm)之间, 含量约 25%; 石英多呈他形充填于长石之间, 少量呈不规则乳滴状穿插于长石中, 含量约 35%, 黑云母呈半自形—他形片状, 含量约 9%; 副矿物为榍石、锆石, 含量约 1%。

达过流纹岩(图 2, 图 3c, 3d): 为下白垩统多尼组中段, 位于达过村附近, 呈近东西向带状出露, 宽约 5.0 km, 厚约 2.5 km。岩石呈浅灰色, 斑状结构, 球粒构造, 斑晶为斜长石、石英, 斜长石呈自形—半自形板状, 部分斜长石边部和微裂隙可见弱绢云母化, 约占全岩的 15%, 石英为他形粒状, 约占全岩的 9%; 基质为隐晶质, 充填于斑晶之间, 多呈显微球粒状, 约占全岩的 75%; 副矿物为锆石、磁铁矿, 含量约为 1%。

达过南流纹岩(图 2, 图 3e, 3f): 为下白垩统多尼组上段, 位于达过村南约 2.5 km 处, 呈近东西向出露, 宽约 1.5 km, 厚约 1.0 km。岩石呈浅灰色, 斑状结构, 流纹构造, 斑晶为斜长石, 呈自形—半自形板状, 斜长石边部和微裂隙可见弱绢云母化, 约占全岩的 10%; 基质为呈流纹状的长英质夹暗色矿物条带, 并具轻微绢云母化, 约占全岩的 89%; 副矿物为

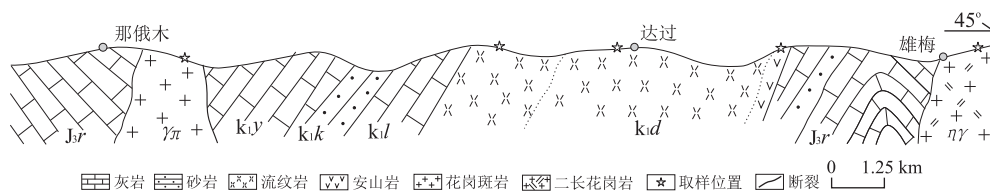


图 2 那俄木—雄梅地质剖面图

Fig.2 The geological section map for Naemu to Xiongmei

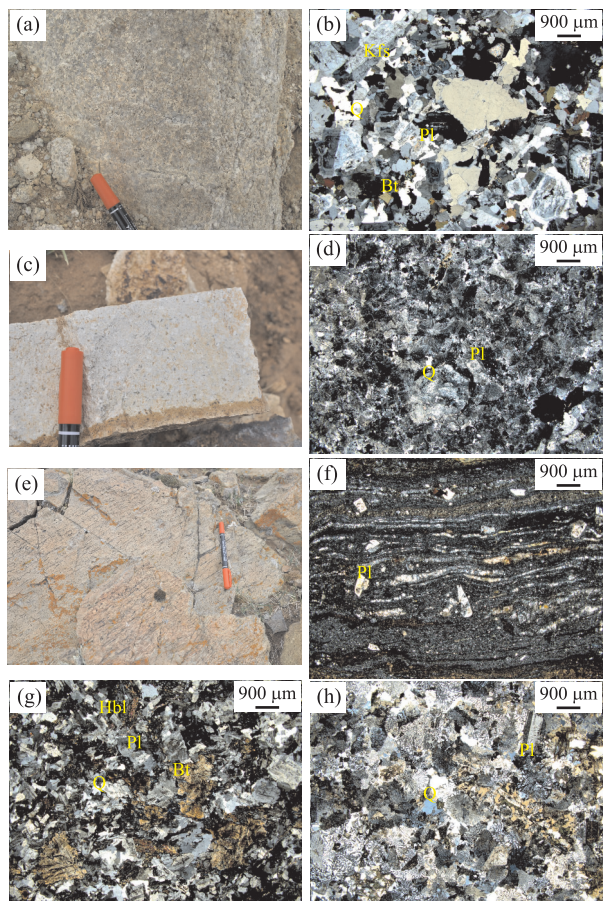


图 3 岩浆岩野外照片和显微照片

Fig. 3 Field pictures and microphotographs for the magmatic rocks

a, b. 黑云母二长花岗岩野外照片(a)和显微照片(正交)(b); c, d. 达过流纹岩野外照片(c)和显微照片(正交)(d); e, f. 达过南流纹岩野外照片(e)和显微照片(正交)(f); g. 安山岩显微照片(正交); h. 花岗斑岩显微照片(正交). Q. 石英; Pl. 斜长石; Kfs. 钾长石; Bt. 黑云母; Hbl. 角闪石

锆石、磁铁矿, 含量约为 1%。

档垌山一达过北安山岩(图 2, 图 3g): 属于下白垩统多尼组的下段, 出露于达过村北约 3.0 km 处, 自档垌山一达过村北呈近东西向展布, 在档垌山宽约 5.0 km, 在达过北宽仅 200.0 m 左右. 岩石呈灰一灰红色, 块状构造, 斑状结构, 显微粒状结构, 斑晶为黑云母、斜长石和角闪石. 黑云母呈半自形片状, 沿微裂隙存在弱绢云母化, 含量约 10%; 斜长石呈自形一半自形板柱状, 含量约 5%; 角闪石呈半自形一他形, 仅残留其晶形, 已强绢云母化、绿泥石化, 并沿裂隙析出少量磁铁矿, 约占 5%; 基质为显微长石和少量石英及黑云母, 约为 79%, 其中石英呈他形显微颗粒填隙物; 部分黑云母边部具弱绿泥石化, 副矿物为锆石、磁铁矿, 含量约为 1%。

那俄木花岗斑岩(图 2, 图 3h): 出露于那俄木北侧, 近圆形, 出露面积约 15 km², 侵入于晚侏罗世灰岩中. 岩石呈浅灰色, 块状构造, 斑状结构, 斑晶为斜长石、石英, 斜长石呈自形一半自形板状, 含量约 5%, 石英呈他形粒状, 含量约 9%; 基质为充填于斑晶之间的显微球粒状和显微不规则状长英质混合物, 约占全岩的 85%; 副矿物为锆石、磁铁矿, 含量约 1%。

3 分析方法

本文采样位置均远离围岩接触带, 并选择侵入岩和火山岩内裂隙不发育、无脉体、无或弱蚀变的部位取样, 室内进一步清洗晾干后, 送河北廊坊区调院进行岩石薄片磨制、粉样加工和单矿物挑选。

全岩化学分析在国家地质实验测试中心完成. 主量元素采用 X-ray 荧光光谱法(Rigaku-3080)分析完成, 分析精度优于 0.5%. 微量元素 Zr、Nb、V、Cr、Sr、Ba、Zn、Ni、Rb 和 Y 使用 XRF 设备 Rigaku-2100 分析, 其他微量元素和稀土元素使用电感耦合等离子体质谱(ICP-MS)进行分析, 当元素含量大于 1×10⁻⁶ 时, 分析精度优于 1%~5%, 当元素含量小于 1×10⁻⁶ 时, 分析精度优于 5%~10%。

挑选纯度在 99% 以上的锆石样品制靶在河北省廊坊区调院完成, 阴极发光照在中国地质科学院离子探针中心完成. LA-ICP-MS 锆石 U-Pb 同位素定年在中国地质大学(武汉)地质过程与矿产资源国家重点实验室完成, 激光剥蚀斑束直径为 32 μm, 激光剥蚀深度为 20~40 μm. 以国际标准锆石 91500 为外标和²⁹Si(锆石中 SiO₂ 的含量为 32.18%)为内标测定锆石中 U、Th 和 Pb 的含量(Hu *et al.*, 2012), 采用 ICPMSDataCal(V3.7)软件对同位素比值数据进行处理(Liu *et al.*, 2010) 和利用 ISOPLLOT 程序进行 U-Pb 加权平均年龄计算及谐和图的绘制(Ludwig, 2003)。

锆石 Hf 同位素测试在中国地质科学院地质研究所大陆构造与动力学重点实验室完成, 试验设备为 Neptune Plus 型多接收等离子质谱和 GeoLas-Pro 193 nm 激光剥蚀系统(LA-MC-ICP-MS), 测试点位依据锆石 U-Pb 同位素分析点位, 剥蚀直径采用 44 μm, 实验过程中采用 He 作为剥蚀物质载气, 测试时使用锆石国际标样 GJ-1 作为参考物质. 相关仪器运行条件及详细分析流程见侯可军等(2007). 分析过程中锆石标准 GJ-1 的¹⁷⁶Hf/¹⁷⁷Hf 测试加权

平均值为 $0.282\ 007 \pm 0.000\ 025$ (2σ), 计算初始 $^{176}\text{Hf}/^{177}\text{Hf}$ 时, Lu 的衰变常数采用 $1.865 \times 10^{-11}\ \text{a}^{-1}$ (Scherer *et al.*, 2001), $\epsilon_{\text{Hf}}(t)$ 值的计算采用球粒陨石 Hf 同位素 $^{176}\text{Lu}/^{177}\text{Hf}=0.033\ 6$, $^{176}\text{Hf}/^{177}\text{Hf}=0.282\ 785$ (Bouvier *et al.*, 2008). 在 Hf 的地幔模式年龄计算中, 亏损地幔 $^{176}\text{Hf}/^{177}\text{Hf}$ 值采用 $0.283\ 25$, $^{176}\text{Lu}/^{177}\text{Hf}$ 值采用 $0.038\ 4$ (Griffin *et al.*, 2000), 地壳模式年龄计算时采用平均地壳的 $^{176}\text{Lu}/^{177}\text{Hf}=0.015$ (Griffin *et al.*, 2000).

4 岩石地球化学特征

本文对永珠地区雄梅黑云母二长花岗岩、那俄木花岗斑岩、达过和达过南流纹岩, 以及档垌山安山岩进行了地球化学分析(表 1). 分析结果显示所采黑云母二长花岗岩、花岗斑岩、达过和达过南流纹岩样品的 CO_2 (0.10~0.45)、 H_2O (0.58~1.46) 和烧失量 (0.47~2.09) 均较低, 可代表岩石的原始组分; 安山岩样品的 CO_2 (0.08~0.92)、 H_2O (2.96~4.50) 和烧失量 (2.87~3.69) 偏高, 应为其弱绿泥石化和绢云母化影响所致, 将不采用它的活动元素探讨岩石成因. 所有样品的主量元素均去除 CO_2 、 H_2O 和烧失量后换算到 100% 再应用.

雄梅黑云母二长花岗岩和那俄木花岗斑岩的 SiO_2 含量在 72.00%~76.68% 之间, K_2O 含量在 3.28%~4.80% 之间, $\text{A}/\text{CNK}=1.06\sim 1.19$, $\text{A}/\text{NK}=1.23\sim 1.45$, 里特曼指数 $\sigma=1.59\sim 1.95$, 为高钾钙碱性过铝—强过铝质花岗岩(图 4a~4c). 岩石的 ΣREE 为 $77.5 \times 10^{-6}\sim 270.7 \times 10^{-6}$, LREE/HREE 在 6.65~20.31 之间, $(\text{La}/\text{Sm})_{\text{N}}=5.34\sim 7.98$, $(\text{Gd}/\text{Yb})_{\text{N}}=1.56\sim 1.93$, $\delta\text{Eu}=0.29\sim 0.58$, 显示为轻稀土富集、分馏程度高, 重稀土分馏程度低, Eu 明显负异常, 稀土球粒陨石标准化配分模式呈右倾的“V”型(图 5a). 微量元素原始地幔标准化蛛网图(图 5b)显示大离子亲石元素 Rb、K 和放射性元素 U、Th 富集, 高场强元素 Nb、P、Ti 和大离子亲石元素 Ba、Sr 明显负异常.

达过和达过南流纹岩的 SiO_2 含量在 70.36%~77.55% 之间, K_2O 含量在 3.93%~4.57% 之间, $\text{A}/\text{CNK}=1.01\sim 1.37$, $\text{A}/\text{NK}=1.29\sim 1.45$, 里特曼指数 $\sigma=1.35\sim 2.00$, 为高钾钙碱性过铝—强过铝质酸性火山岩(图 4a~4c). 流纹岩的 ΣREE 为 $168.3 \times 10^{-6}\sim 310.9 \times 10^{-6}$, LREE/HREE 在 17.05~22.23 之间, $(\text{La}/\text{Sm})_{\text{N}}=4.92\sim 5.81$, $(\text{Gd}/\text{Yb})_{\text{N}}=1.60\sim$

2.02, $\delta\text{Eu}=0.30\sim 0.44$, 为轻稀土相对富集和分馏程度略高, 重稀土分馏程度低, Eu 明显负异常, 稀土球粒陨石标准化配分模式呈右倾的“V”型(图 5c). 微量元素原始地幔标准化蛛网图(图 5d)显示大离子亲石元素 Rb、K 和放射性元素 U、Th 相对原始地幔强富集, 高场强元素 Nb、P、Ti 和大离子亲石元素 Ba、Sr 明显亏损.

安山岩的后期蚀变对其常量组分和大离子活泼元素影响较大(仅作参考), 而稀土元素和高场强元素较为稳定, 基本不受后期蚀变的影响. 岩石中 SiO_2 含量在 57.37%~58.45% 之间, K_2O 含量在 3.93%~4.57% 之间, MgO 含量在 4.43%~4.70% 之间, 里特曼指数 $\sigma=1.27\sim 2.80$, $\text{Mg}^{\#}=56.66\sim 57.52$, 反映其为高钾钙碱性岩浆岩(图 4a, 4b). 安山岩的 ΣREE 为 $87.9 \times 10^{-6}\sim 116.7 \times 10^{-6}$, LREE/HREE 在 6.88~8.07 之间, $(\text{La}/\text{Sm})_{\text{N}}=5.62\sim 7.39$, $(\text{Gd}/\text{Yb})_{\text{N}}=2.05\sim 2.14$. 除 13DB-67 的 δEu 为 1.09 外, 其他分布于 0.64~0.74 之间, 为轻稀土相对富集和分馏程度高, Eu 弱负异常, 稀土球粒陨石标准化配分模式呈右倾的“V”型(图 5c). 微量元素原始地幔标准化蛛网图(图 5d)显示大离子亲石元素 Rb、K 和放射性元素 Th 相对原始地幔略富集, 高场强元素 Nb、Ta、P、Ti 和大离子亲石元素 Sr, 以及放射性元素 U 相对亏损.

5 锆石 LA-ICP-MS U-Pb 定年和 Hf 同位素组成

5.1 锆石 LA-ICP-MS U-Pb 定年

黑云母二长花岗岩(16QXS-2)的锆石无色透明, 自形一半自形短柱状, 粒度在 $(50\ \mu\text{m} \times 60\ \mu\text{m})\sim(50\ \mu\text{m} \times 150\ \mu\text{m})$ 之间, 长宽比约 1:1~2:1, 具典型岩浆锆石韵律环带(图 6a), 锆石的 Th/U 比值为 0.5~1.1, 为岩浆成因锆石特征 (Corfu *et al.*, 2003; Hoskin and Schaltegger, 2003; 吴元保和郑永飞, 2004). 点 16QXS-2-1 和 16QXS-2-9 获得数据的谐和度过低(分别为 41% 和 53%), 不参与本次年龄的计算, 剩余 18 颗锆石的 U-Pb 加权平均年龄为 $118 \pm 1.0\ \text{Ma}$ ($\text{MSWD}=1.3$) (表 2, 图 7a), 代表锆石结晶年龄.

流纹岩(16QXS-30)的锆石为浅灰—浅黄—无色透明, 自形一半自形短柱状, 长约 $(50\ \mu\text{m} \times 50\ \mu\text{m})\sim(60\ \mu\text{m} \times 120\ \mu\text{m})$, 长宽比约 1:1~

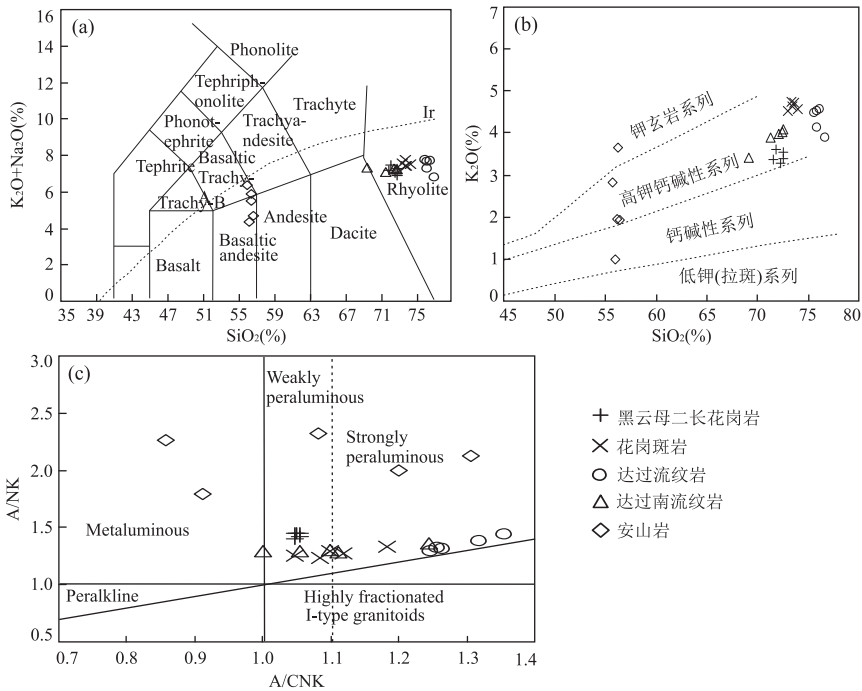


图 4 $K_2O+Na_2O-SiO_2$ 火山岩分类命名图(a), K_2O-SiO_2 钙碱性判别图(b)和 A/NK-A/CNK 图解(c)

Fig.4 $K_2O+Na_2O-SiO_2$ volcanics classification diagram (a), K_2O-SiO_2 calc-alkaline discriminant diagram (b) and A/NK-A/CNK diagram (c)

图 a 据 Rickwood(1989);图 b 据 Peccerillo and Taylor(1976);图 c 据 Maniar and Piccoli(1989)

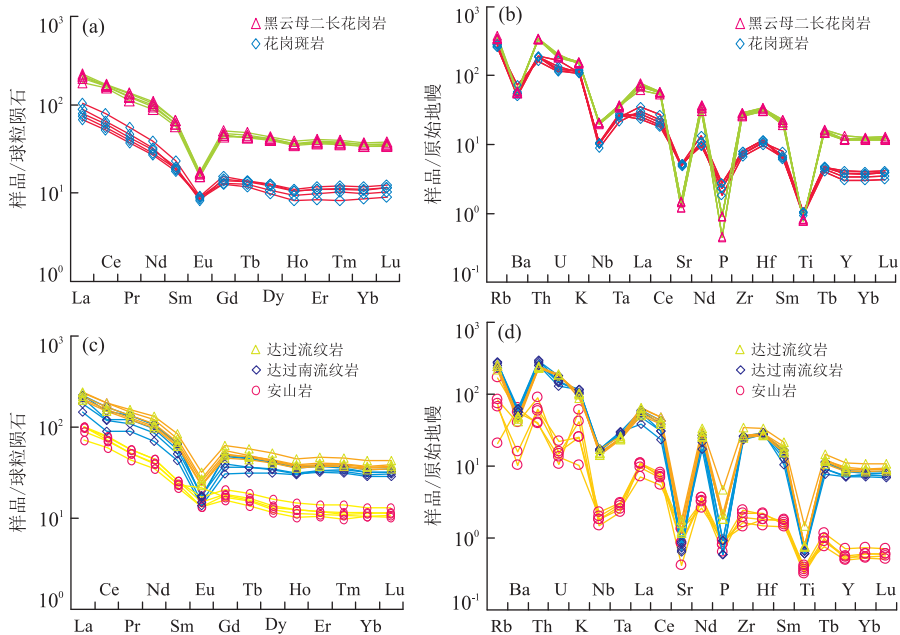


图 5 岩浆岩稀土元素球粒陨石标准化配分模式(a,c)和微量元素原始地幔标准化蛛网图(b,d)

Fig.5 Chondrite-normalized REE patterns (a,c) and primitive mantle-normalized trace element spider diagrams (b,d) for the magmatic rocks

标准化值据 Sun and McDonough(1989)

2.2 : 1, 锆石的 Th/U 比值为 0.6~1.0, 韵律环带清晰(图 6b), 为岩浆成因锆石特征(Corfu *et al.*, 2003; Hoskin and Schaltegger, 2003; 吴元保和郑永

飞, 2004). 点 16QXS-30-17 获得数据的谐和度过低(7%), 不参与本次年龄的计算, 剩余 19 颗锆石的 U-Pb 加权平均年龄为 121 ± 0.8 Ma (MSWD=1.1)



图 6 黑云母二长花岗岩(a)、流纹岩(b)和安山岩(c)锆石阴极发光照片

Fig. 6 Cathodoluminescence images of zircons for the biotite-monzonitic granites (a), rhyolites (b) and andesite (c)

(表 2, 图 7b), 代表锆石结晶年龄。

安山岩(13DB-69)的锆石浅灰—浅黄色, 自形一半自形短柱状(图 6c), 长约(40 μm × 50 μm) ~ (60 μm × 125 μm), 长宽比约 1.5 : 1 ~ 2.5 : 1, 锆石的 Th/U 比值为 0.9 ~ 1.6, 为岩浆成因锆石特征 (Corfu *et al.*, 2003; Hoskin and Schaltegger, 2003; 吴元保和郑永飞, 2004)。共计 20 颗锆石的 U-Pb 加权平均年龄为 115 ± 0.8 Ma (MSWD = 2.7) (表 2, 图 7c), 为锆石结晶年龄。

5.2 Hf 同位素

雄梅黑云母二长花岗岩体(16QXS-2)和达过南流纹岩(16QXS-30)中的锆石 Hf 同位素分析结果表明, 雄梅黑云母二长花岗岩体 20 颗锆石的 $^{176}\text{Yb}/^{177}\text{Hf}$ 和 $^{176}\text{Lu}/^{177}\text{Hf}$ 的比值范围分别为 0.015 774 ~ 0.079 642 和 0.000 546 ~ 0.002 385, $^{176}\text{Hf}/^{177}\text{Hf}$ 范围为 0.282 681 ~ 0.282 69, 对应的 $\epsilon_{\text{Hf}}(t)$ 变化于 -1.21 ~ 3.01 (表 3), 峰值为 -1.0 ~ -1.0 (图 8a), 二阶段模式年龄 (t_{DM2}) 为 0.99 ~ 1.26 Ga 之间, 集中分布于 1.1 ~ 1.3 Ga (图 8b)。

达过南流纹岩(16QXS-30)的 20 颗锆石的 $^{176}\text{Yb}/^{177}\text{Hf}$ 和 $^{176}\text{Lu}/^{177}\text{Hf}$ 比值范围分别为 0.043 807 ~ 0.103 238 和 0.001 184 ~ 0.002 678, $^{176}\text{Hf}/^{177}\text{Hf}$ 范围为 0.282 685 ~ 0.282 850, 对应的 $\epsilon_{\text{Hf}}(t)$ 变化于 -0.68 ~ 5.35 (表 3), 峰值为 -1.0 ~

3.0 (图 8a), 二阶段模式年龄 (t_{DM2}) 为 0.84 ~ 1.22 Ga 之间, 集中分布于 0.9 ~ 1.2 Ga (图 8b)。

6 讨论

6.1 岩浆形成的构造环境

研究表明, 岛弧火山岩以拉斑玄武岩系列的玄武岩、玄武安山岩, 以及钙碱性系列的安山岩和英安岩为主 (Miyashiro, 1974), 侵入岩以闪长岩、奥长花岗岩、英云闪长岩和花岗闪长岩为主 (Maniar and Piccoli, 1989; 邓晋福等, 2007); 活动大陆边缘弧火山岩以高钾钙碱性系列的安山岩、英安岩和流纹岩为主 (Miyashiro, 1974), 侵入岩以花岗闪长岩、二长花岗岩为主 (Maniar and Piccoli, 1989; 邓晋福等, 2007)。永珠地区分布的火山岩以流纹岩、英安岩和安山岩为主, 局部出露少量玄武岩, 侵入岩为二长花岗岩、花岗斑岩和少量花岗闪长岩 (董永胜等, 2012, 西藏 1 : 50 000 青卡尔等四幅区域地质调查; 刘振宇等, 2015, 西藏 1 : 50 000 雄梅镇等四幅区域地质调查报告), 地球化学研究显示区内黑云母二长花岗岩、花岗斑岩、流纹岩和安山岩均为高钾钙碱性岩浆岩, 与活动大陆边缘弧岩浆岩的岩石组合和岩石系列一致; 而且中—酸性岩浆岩亏损高场强元素 Nb、Ta、P、Ti 和大离子亲石元素 Ba、Sr, 富集大离子亲石元素 Rb、K 和放射性元素 U、Th, 与亏损高场强元素富集大离子亲石元素的典型岛弧岩浆岩存在差异, 而与亏损 Nb、Ta、Ti、Ba、Sr 的大陆边缘弧岩浆岩的特征一致 (Pearce *et al.*, 1984; Hall, 1989; McCulloch and Gamble, 1991; Pearce, 1996; Tuner *et al.*, 1996; Miller *et al.*, 1999); 对比研究区内早白垩世的岩浆岩, 本文研究岩浆岩的岩石矿物组成未发现碱性矿物, 地球化学也未显示高的 $\text{K}_2\text{O} + \text{Na}_2\text{O}$ 和 FeO^{T} 含量, 与曲晓明等 (2012) 在该地区发现形成于拉萨—羌塘地体碰撞后伸展环境的 A 型花岗岩不同, 而与康志强等 (2009) 认为的班公湖—怒江洋俯冲的弧花岗岩相似; 同时, 在 Muller and Grovers (1994) 构造判别图解的 Y-Zr 图解中, 黑云母二长花岗岩投点落入与弧相关区, 花岗斑岩和流纹岩落入板内靠近与弧相关区 (图 9a), Zr/Al₂O₃-Ti₂O/Al₂O₃ 图解中所有点均落入与弧相关的大陆和碰撞后环境 (图 9b), Gorton and Schandl (2000) 的 Th/Yb-Ta/Yb 构造图解中, 所有样点均落入大陆活动边缘 (图 9c), 安山岩的 La/Yb-Sc/Ni 构造图解中, 本文的安山岩落入大陆边缘弧内

表 2 黑云母二长花岗岩与流纹岩 LA-ICP-MS 锆石 U-Pb 定年结果

Table 2 LA-ICP-MS zircon U-Pb dating results for the biotite-monzonitic granites, rhyolites and andesites

测点	Pb (10^{-6})	Th (10^{-6})	U (10^{-6})	Th/U	同位素						年龄(Ma)	
					$^{207}\text{Pb}/^{206}\text{Pb}$		$^{207}\text{Pb}/^{235}\text{U}$		$^{206}\text{Pb}/^{238}\text{U}$		$^{206}\text{Pb}/^{238}\text{U}$	
						1 σ		1 σ		1 σ		1 σ
16QXS-2, 雄梅黑云母二长花岗岩, 北纬: 31°24'1.2", 东经: 89°00'25.8"												
1	205	1970	1841	1.1	0.092 7	0.004 5	0.227 3	0.010 9	0.017 8	0.000 2	114	1.4
2	270	2 709	2 768	1.0	0.047 9	0.001 5	0.125 7	0.004 2	0.019 0	0.000 3	121	1.6
3	99	1 089	1 254	0.9	0.050 0	0.002 4	0.126 2	0.006 2	0.018 2	0.000 2	116	1.3
4	229	2 527	2 176	1.2	0.046 8	0.001 7	0.119 8	0.004 4	0.018 6	0.000 2	119	1.5
5	30	262	539	0.5	0.060 0	0.003 6	0.153 1	0.009 3	0.018 7	0.000 3	119	1.9
6	59	536	948	0.6	0.048 2	0.002 4	0.119 9	0.005 9	0.018 2	0.000 3	116	1.9
7	62	595	870	0.7	0.048 5	0.002 6	0.123 6	0.006 3	0.018 7	0.000 3	120	1.8
8	33	294	484	0.6	0.060 8	0.003 6	0.159 1	0.009 5	0.018 9	0.000 3	120	2.1
9	86	602	1101	0.6	0.077 8	0.005 3	0.227 1	0.019 0	0.020 2	0.000 3	129	2.2
10	36	328	641	0.5	0.057 0	0.004 1	0.141 3	0.009 1	0.018 2	0.000 3	116	1.9
11	101	1 080	1 189	0.9	0.048 5	0.002 3	0.124 7	0.005 6	0.018 9	0.000 3	121	1.8
12	196	1 873	2 289	0.8	0.053 5	0.002 1	0.144 9	0.006 5	0.019 3	0.000 3	123	1.9
13	76	747	1 020	0.7	0.049 8	0.002 6	0.126 8	0.006 5	0.018 6	0.000 3	119	1.6
14	190	1 953	2 415	0.8	0.049 9	0.002 3	0.126 7	0.005 8	0.018 3	0.000 2	117	1.5
15	245	2 639	2 538	1.0	0.049 9	0.002 0	0.125 6	0.005 3	0.018 1	0.000 2	116	1.6
16	68	998	984	1.0	0.062 3	0.003 6	0.158 8	0.008 8	0.018 6	0.000 3	119	1.8
17	75	736	1 081	0.7	0.049 2	0.002 2	0.124 1	0.005 5	0.018 4	0.000 3	118	1.7
18	102	972	1 238	0.8	0.048 5	0.002 4	0.123 7	0.006 2	0.018 4	0.000 3	118	1.6
19	144	1 448	1 606	0.9	0.049 6	0.002 2	0.124 2	0.005 4	0.018 2	0.000 2	116	1.4
20	107	1 069	1 378	0.8	0.048 4	0.002 6	0.122 8	0.006 6	0.018 6	0.000 3	119	1.7
16QXS-30, 达过南流纹岩, 北纬: 31°19'45.0", 东经: 88°54'51.6"												
1	152	1 486	1 861	0.8	0.048 4	0.002 2	0.124 3	0.005 4	0.018 8	0.000 3	120	1.6
2	57	517	923	0.6	0.052 0	0.002 6	0.136 9	0.007 1	0.019 0	0.000 3	122	2.0
3	81	765	1 254	0.6	0.059 7	0.003 0	0.154 2	0.007 3	0.019 0	0.000 3	122	2.1
4	92	888	1 262	0.7	0.054 6	0.002 5	0.135 3	0.005 5	0.018 5	0.000 3	118	1.8
5	65	590	1 026	0.6	0.053 9	0.003 0	0.142 5	0.007 6	0.019 2	0.000 3	123	2.1
6	109	967	1 389	0.7	0.053 3	0.002 7	0.140 1	0.006 8	0.019 3	0.000 3	123	2.0
7	113	1 020	1 451	0.7	0.051 7	0.002 4	0.137 6	0.006 1	0.019 5	0.000 3	124	2.1
8	139	1 343	1 876	0.7	0.052 1	0.002 2	0.134 6	0.005 5	0.018 9	0.000 3	121	1.6
9	77	743	1 179	0.6	0.050 1	0.002 8	0.128 1	0.006 9	0.019 0	0.000 4	121	2.3
10	143	1 384	1 693	0.8	0.054 5	0.002 5	0.143 4	0.006 3	0.019 3	0.000 3	123	1.8
11	93	859	1 255	0.7	0.049 1	0.002 6	0.128 8	0.006 9	0.019 2	0.000 3	122	1.9
12	1 040	1 049	1 548	0.7	0.052 6	0.002 4	0.132 4	0.006 3	0.018 2	0.000 3	116	1.8
13	137	1 313	1 795	0.7	0.050 5	0.002 3	0.130 9	0.005 7	0.019 1	0.000 3	122	1.8
14	72	670	1 079	0.6	0.054 2	0.002 9	0.135 0	0.006 8	0.018 5	0.000 3	118	2.0
15	86	818	1 244	0.7	0.050 5	0.002 4	0.129 4	0.005 7	0.018 9	0.000 3	121	2.0
16	265	2 739	2 856	1.0	0.049 5	0.002 1	0.124 6	0.005 2	0.018 6	0.000 3	119	1.8
17	136	689	1 128	0.6	0.117 4	0.012 8	0.432 2	0.059 9	0.021 1	0.000 6	135	3.6
18	133	1 317	1 595	0.8	0.046 1	0.002 2	0.120 9	0.005 8	0.019 1	0.000 3	122	1.8
19	107	1 056	1 531	0.7	0.051 1	0.002 6	0.131 8	0.006 4	0.018 9	0.000 3	121	1.7
20	148	1 525	1 733	0.9	0.052 4	0.002 2	0.136 0	0.005 6	0.019 1	0.000 3	122	1.8
13DB-69, 安山岩, 北纬: 31°20'26.0", 东经: 88°50'21.7"												
1	117	4 214	4 408	1.0	0.047 7	0.001 3	0.116 7	0.003 0	0.017 6	0.000 1	113	0.9
2	98	3 664	3 748	1.0	0.046 7	0.001 4	0.115 7	0.003 5	0.017 9	0.000 2	115	1.3
3	81	2 916	3 032	1.0	0.047 2	0.001 6	0.118 2	0.004 1	0.018 0	0.000 2	115	1.1
4	130	4 627	4 976	0.9	0.048 9	0.001 3	0.120 3	0.003 3	0.017 7	0.000 1	113	0.9
5	195	9 321	6 009	1.6	0.047 5	0.001 1	0.118 0	0.002 8	0.018 0	0.000 1	115	0.9
6	171	7 463	5 426	1.4	0.046 8	0.001 1	0.119 4	0.002 8	0.018 5	0.000 2	118	1.1
7	200	9 878	6 218	1.6	0.045 0	0.001 0	0.111 4	0.002 4	0.017 9	0.000 1	114	0.9
8	162	6 810	5 335	1.3	0.048 1	0.001 2	0.123 5	0.003 1	0.018 5	0.000 2	118	1.0
9	85	3 053	3 083	1.0	0.048 1	0.001 5	0.121 8	0.003 9	0.018 3	0.000 2	117	1.1
10	139	5 859	4 835	1.2	0.045 9	0.001 3	0.112 9	0.003 0	0.017 8	0.000 2	114	1.0
11	128	5 333	4 069	1.3	0.049 4	0.001 6	0.126 2	0.003 9	0.018 4	0.000 2	118	1.2
12	188	8 161	5 901	1.4	0.050 9	0.001 6	0.128 2	0.004 1	0.018 0	0.000 1	115	0.9
13	228	8 556	7 734	1.1	0.048 4	0.001 1	0.121 8	0.002 8	0.018 0	0.000 2	115	1.0
14	165	6 365	5 272	1.2	0.047 4	0.001 3	0.122 1	0.003 4	0.018 5	0.000 2	118	1.2
15	246	9 873	8 337	1.2	0.051 4	0.001 4	0.127 3	0.003 5	0.017 8	0.000 2	113	1.0
16	184	7 479	6 178	1.2	0.047 2	0.001 2	0.116 9	0.002 9	0.017 8	0.000 2	114	1.0
17	147	5 978	4 806	1.2	0.046 7	0.001 4	0.117 4	0.003 4	0.018 1	0.000 2	116	1.1
18	127	4 749	4 619	1.0	0.049 6	0.001 6	0.122 5	0.003 9	0.017 8	0.000 2	114	1.1
19	249	11 144	7 966	1.4	0.050 9	0.001 0	0.127 9	0.002 6	0.018 0	0.000 1	115	0.9
20	276	12 332	8 893	1.4	0.048 7	0.001 2	0.122 1	0.003 0	0.018 0	0.000 2	115	1.1

注: 测试单位为 中国地质大学(武汉)地质过程与矿产资源国家重点实验室。

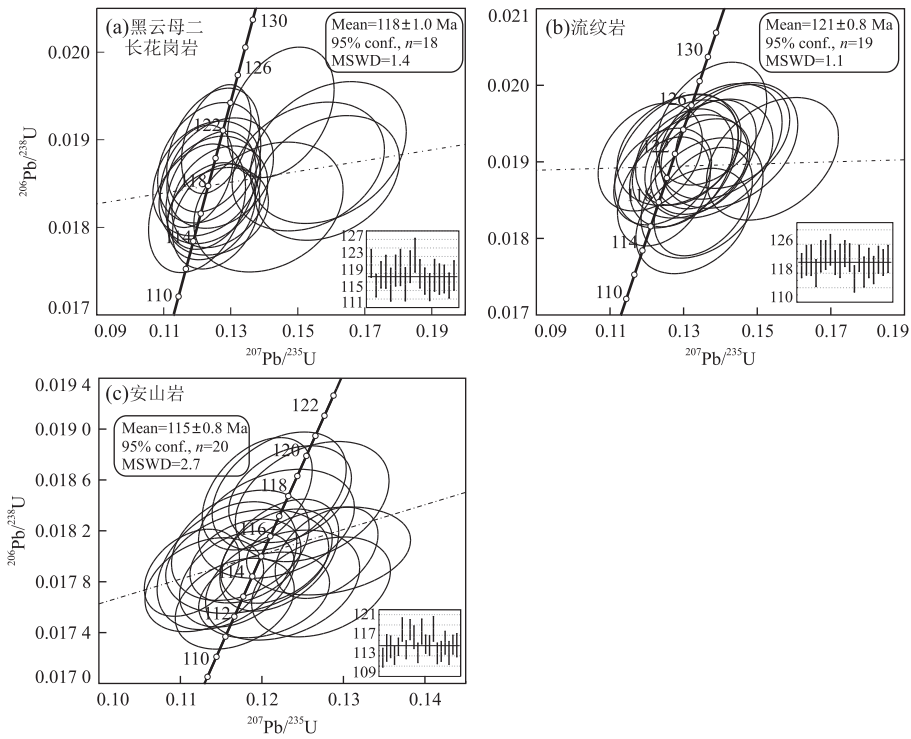


图 7 黑云母二长花岗岩、流纹岩和安山岩锆石 U-Pb 年龄谐和图

Fig.7 Zircon LA-ICP-MS concordia diagrams for the biotite-monzonitic granites, hyolites and andesite

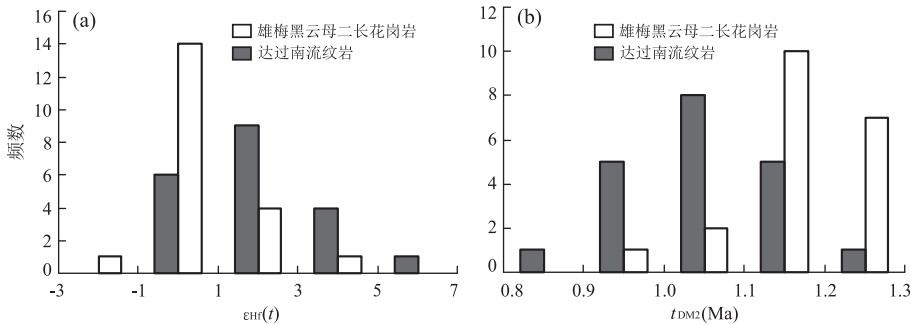


图 8 黑云母二长花岗岩和流纹岩锆石 $\epsilon_{\text{Hf}}(t)$ (a) 和 t_{DM2} 直方图(b)

Fig.8 Histogram $\epsilon_{\text{Hf}}(t)$ (a) of and t_{DM2} for the biotite-monzonitic granite and rhyolite (b)

(图 9d),也进一步佐证了本文研究岩浆岩形成于大陆边缘弧环境.所研究的火山岩赋存于早白垩世多巴组和多巴组之间的滨—浅海相灰岩之间(图 2a,曲永贵等,2003,多巴幅 1:25 万区域地质调查报告;董永胜等,2012,西藏 1:50 000 青卡尔等四幅区域地质调查;刘振宇等,2015,西藏 1:50 000 雄梅镇等四幅区域地质调查报告),也一定程度上反映了其形成时该地区处于陆缘海环境.综上,笔者认为永珠地区早白垩世岩浆岩形成于大陆边缘弧环境.

拉萨地体位于班公湖—怒江缝合带和雅鲁藏布江缝合带之间,位于拉萨地体北缘的永珠地区早白垩世岩浆岩是形成于班公湖—怒江中特提斯洋的陆缘弧?还是雅鲁藏布江新特提斯洋的陆缘弧?探讨

如下:近年来古地磁研究表明,自 110 Ma 以来,拉萨地块南北缩短了约 870 km(Chen *et al.*, 2012),早白垩世后拉萨地块存在最大达 60%的地壳缩短(Murphy *et al.*, 1997;Zhang *et al.*, 2004),现今的地理位置,雅鲁藏布江缝合带距拉萨北部约 200 km,按此推算早白垩世期间本文研究区和雅鲁藏布江缝合带相距不少于 600 km(Kapp *et al.*, 2007;Leier *et al.*, 2007),而且雅鲁藏布江新特提斯洋壳在早白垩世(130~110 Ma)刚开始北向俯冲(Sengör *et al.*, 1988;Niu *et al.*, 2003;Yang *et al.*, 2011),尚不能使远在拉萨地体北缘的永珠地区产生岩浆活动,即使雅鲁藏布江新特提斯洋壳北向俯冲引发了永珠地区早白垩世的岩浆活动,也只能

表 3 黑云母二长花岗岩与流纹岩 LA-ICP-MS 锆石 Hf 同位素

Table 3 LA-ICP-MS zircon Hf isotopic compositions for the biotite-monzonitic granites and rhyolites

测点	<i>t</i> (Ma)	¹⁷⁶ Yb/ ¹⁷⁷ Hf	2σ	¹⁷⁶ Lu/ ¹⁷⁷ Hf	2σ	¹⁷⁶ Hf/ ¹⁷⁷ Hf	2σ	(¹⁷⁶ Hf/ ¹⁷⁷ Hf) _i	ε _{Hf} (<i>t</i>)	2σ	<i>t</i> _{DM} (Ma)	<i>t</i> _{DM2} (Ma)
16QXS-2, 雄梅黑云母二长花岗岩, 北纬: 31°24'1.2", 东经: 89°00'25.8"												
1	114	0.036 461	0.001 010	0.001 169	0.000 028	0.282 707	0.000 020	0.282 70	0.10	0.7	776	1 168
2	121	0.037 299	0.000 345	0.001 210	0.000 013	0.282 691	0.000 018	0.282 69	-0.29	0.6	799	1 198
3	116	0.038 094	0.000 479	0.001 156	0.000 012	0.282 727	0.000 022	0.282 72	0.86	0.8	747	1 121
4	119	0.079 642	0.001 108	0.002 385	0.000 021	0.282 769	0.000 024	0.282 76	2.33	0.9	710	1 029
5	119	0.015 774	0.000 126	0.000 546	0.000 005	0.282 714	0.000 019	0.282 71	0.50	0.7	754	1 146
6	116	0.036 725	0.000 375	0.001 169	0.000 009	0.282 703	0.000 019	0.282 70	0.02	0.7	781	1 174
7	120	0.046 230	0.000 383	0.001 442	0.000 015	0.282 687	0.000 019	0.282 68	-0.48	0.7	810	1 209
8	120	0.016 645	0.000 310	0.000 519	0.000 009	0.282 728	0.000 016	0.282 73	1.04	0.6	733	1 112
9	129	0.046 223	0.001 448	0.001 408	0.000 038	0.282 705	0.000 019	0.282 70	0.34	0.7	783	1 164
10	116	0.043 546	0.000 774	0.001 351	0.000 025	0.282 738	0.000 020	0.282 74	1.25	0.7	735	1 096
11	121	0.023 725	0.000 530	0.000 737	0.000 015	0.282 694	0.000 016	0.282 69	-0.17	0.6	785	1 190
12	123	0.066 133	0.000 291	0.001 905	0.000 010	0.282 785	0.000 026	0.282 78	3.01	0.9	678	989
13	119	0.042 184	0.001 249	0.001 268	0.000 038	0.282 719	0.000 018	0.282 72	0.63	0.6	761	1 138
14	117	0.054 206	0.000 586	0.001 622	0.000 017	0.282 688	0.000 025	0.282 68	-0.54	0.9	813	1 210
15	116	0.070 765	0.000 333	0.002 069	0.000 009	0.282 681	0.000 027	0.282 68	-0.82	1.0	832	1 228
16	119	0.047 068	0.001 254	0.001 399	0.000 033	0.282 667	0.000 020	0.282 66	-1.21	0.7	837	1 255
17	118	0.047 984	0.000 494	0.001 476	0.000 017	0.282 681	0.000 021	0.282 68	-0.73	0.7	819	1 224
18	118	0.047 668	0.000 291	0.001 399	0.000 006	0.282 685	0.000 024	0.282 68	-0.61	0.9	812	1 215
19	116	0.060 173	0.001 098	0.001 705	0.000 032	0.282 751	0.000 021	0.282 75	1.66	0.7	724	1 069
20	119	0.056 144	0.001 278	0.001 585	0.000 023	0.282 703	0.000 021	0.282 70	0.05	0.8	790	1 175
16QXS-30, 达过南流纹岩, 北纬: 31°19'45.0", 东经: 88°54'51.6"												
1	120	0.069 559	0.000 732	0.002 117	0.000 026	0.282 762	0.000 021	0.282 76	2.12	0.7	715	1 043
2	122	0.057 569	0.000 179	0.001 579	0.000 009	0.282 791	0.000 025	0.282 79	3.22	0.9	664	974
3	122	0.059 568	0.000 439	0.001 568	0.000 007	0.282 821	0.000 024	0.282 82	4.29	0.9	620	906
4	118	0.061 923	0.000 911	0.001 568	0.000 016	0.282 768	0.000 021	0.282 76	2.33	0.7	696	1 028
5	123	0.056 145	0.000 321	0.001 429	0.000 007	0.282 850	0.000 025	0.282 85	5.35	0.9	576	839
6	123	0.059 090	0.000 402	0.001 586	0.000 007	0.282 714	0.000 020	0.282 71	0.50	0.7	775	1 149
7	124	0.052 012	0.000 087	0.001 415	0.000 004	0.282 749	0.000 023	0.282 75	1.78	0.8	721	1 068
8	121	0.082 878	0.000 401	0.002 100	0.000 010	0.282 784	0.000 024	0.282 78	2.92	0.8	683	992
9	121	0.050 961	0.000 794	0.001 480	0.000 006	0.282 728	0.000 019	0.282 72	0.97	0.7	753	1 117
10	123	0.094 749	0.000 387	0.002 533	0.000 011	0.282 740	0.000 022	0.282 73	1.37	0.8	756	1 093
11	122	0.058 793	0.000 441	0.001 709	0.000 011	0.282 757	0.000 023	0.282 75	2.01	0.8	715	1 051
12	116	0.062 897	0.000 313	0.001 701	0.000 011	0.282 685	0.000 019	0.282 68	-0.68	0.7	819	1 219
13	122	0.091 275	0.000 070	0.002 402	0.000 003	0.282 752	0.000 024	0.282 75	1.77	0.9	736	1 067
14	118	0.045 915	0.000 581	0.001 266	0.000 008	0.282 766	0.000 022	0.282 76	2.27	0.8	694	1 032
15	121	0.043 807	0.000 290	0.001 184	0.000 003	0.282 712	0.000 019	0.282 71	0.43	0.7	769	1 152
16	119	0.082 996	0.000 211	0.002 304	0.000 005	0.282 760	0.000 023	0.282 75	1.99	0.8	723	1 050
17	135	0.053 274	0.000 356	0.001 722	0.000 009	0.282 798	0.000 028	0.282 79	3.73	1.0	656	952
18	122	0.075 221	0.000 372	0.002 024	0.000 006	0.282 794	0.000 019	0.282 79	3.30	0.7	667	969
19	121	0.103 238	0.000 792	0.002 678	0.000 014	0.282 727	0.000 020	0.282 72	0.85	0.7	779	1 125
20	122	0.060 721	0.000 705	0.001 610	0.000 006	0.282 701	0.000 020	0.282 70	0.04	0.7	793	1 177

注: 测试单位为中国地质科学院地质研究所大陆构造与动力学重点实验室.

形成与洋壳平缓俯冲相关的埃达克岩 (Gutscher *et al.*, 2000). 然而永珠地区早白垩世岩浆岩 (表 1, 图 5) 并不具埃达克岩高 Sr ($>400 \times 10^{-6}$)、贫 Y 和 Yb ($Y \leq 18 \times 10^{-6}$, $Yb \leq 1.9 \times 10^{-6}$) 和无负 Eu 异常 (或有轻微的负 Eu 异常) 特征 (Defant and Drummond, 1990; 王焰等, 2000; Xu *et al.*, 2000; 张旗等, 2002), 因此, 永珠地区早白垩世岩浆岩不是形成于

雅鲁藏布江新特提斯洋壳俯冲的大陆边缘弧. 现今的班公湖—怒江缝合带与拉萨地体北部的永珠地区相距约 100 km, 按早白垩世后拉萨地块存在最大达 60% 的地壳缩短 (Murphy *et al.*, 1997; Zhang *et al.*, 2004) 推算, 早白垩世班公湖—怒江特提斯洋与永珠地区的距离不超过 250 km, 同时, 班公湖—怒江中特提斯洋晚侏罗世已开始俯冲消减 (潘桂棠等,

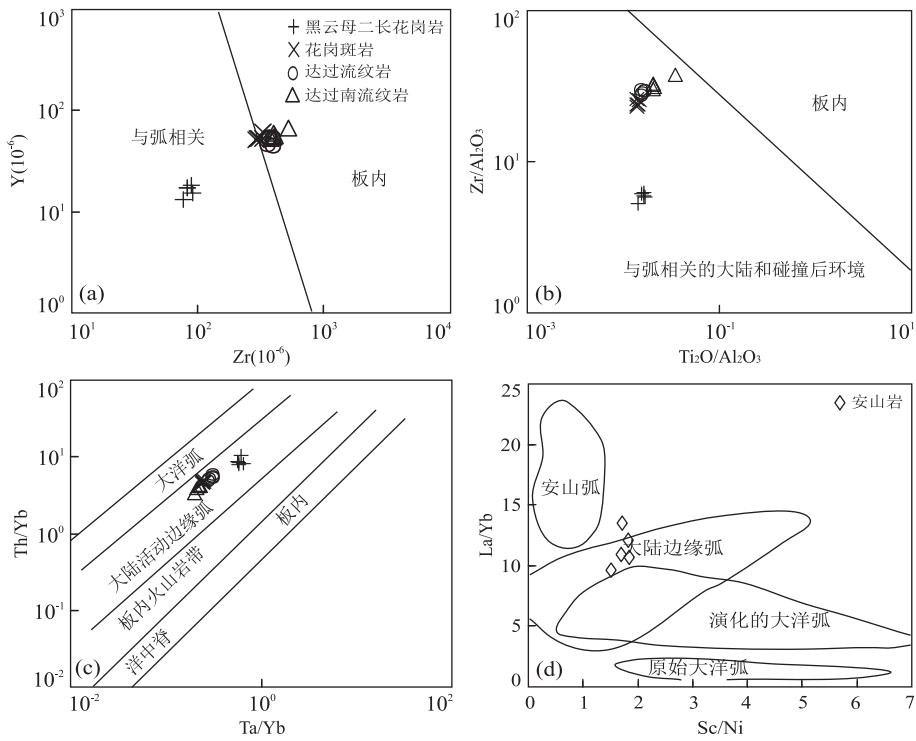


图 9 永珠地区岩浆岩 Y-Zr (a)、Zr/Al₂O₃-TiO₂/Al₂O₃ (b)、Th/Yb-Ta/Yb (c)、La/Yb-Sc/Ni (d) 构造判别图解

Fig.9 Y-Zr (a), Zr/Al₂O₃-TiO₂/Al₂O₃ (b), Th/Yb-Ta/Yb (c) and La/Yb-Sc/Ni (d) discrimination diagrams of tectonic setting for magmatic rocks of Yongzhu region

图 a, b 据 Muller and Groves(1994);图 c 据 Gorton and Schandl(2000);图 d 据 Pearce(1982)

2006; Li *et al.*, 2014b; Hao *et al.*, 2016; Wang *et al.*, 2016), 早白垩世中早期该洋壳应已俯冲至足以引发弧岩浆活动的 120~150 km 的深度 (Crosson and Owens, 1987), 而且, 本文所研究的岩浆岩与以往地质工作者研究的拉萨地体北部与班公湖-怒江特提斯洋壳南向俯冲有关的早白垩世岩浆岩具有相似的锆石 U-Pb 年代学、地球化学和 Hf 同位素特征 (朱弟成等, 2008; Zhu *et al.*, 2011, 2016; 胡隽等, 2014; 李小波等, 2015). 以往研究根据东巧-日土地区分布的晚侏罗世-早白垩世早期的沙木罗组和东巧组与蛇绿岩和木嘎岗日群混杂岩之间的不整合接触 (余光明和王成善, 1990; 王建平等, 2002; 陈国荣等, 2004), 认为班公湖-怒江洋在晚侏罗世-早白垩世已关闭 (Metcalf, 1998, 2013; Yin and Harrison, 2000; Kapp *et al.*, 2003; 莫宣学和潘桂棠, 2006), 鉴于此, 大多研究者采用拉萨-羌塘地体碰撞后俯冲大洋板片断离引发幔源物质上涌继而引发岩浆活动, 来解释拉萨地体北部早白垩世 (134~108 Ma) 大规模具弧岩浆特征的岩浆岩成因 (Zhu *et al.*, 2009, 2011, 2013, 2016; 康志强等, 2009; 陈越等, 2010; 高顺宝等, 2011a; 黄瀚霄等, 2012; Sui *et al.*, 2013; Chen *et al.*, 2014; 关俊雷等, 2014; 孙赛

军等, 2015), 班公-怒江特提斯洋壳南向俯冲消减过程中反而未形成大规模的岩浆活动, 这与现今大洋两侧俯冲带存在大规模的弧岩浆岩事实不太相符. 近年来的地质调查和研究表明, 晚侏罗世-早白垩世早期沙木罗组和东巧组主要分布在班公湖-怒江缝合带北侧局部地区, 而且其下伏不整合接触的蛇绿岩均为 SSZ 型, 该不整合是班公湖-怒江洋北侧弧-弧、弧-陆碰撞关闭的沉积响应, 并不代表班公湖-怒江洋主体洋盆的关闭 (Fan *et al.*, 2014), 广泛分布于班公湖-怒江缝合带上的早白垩世末期河湖相沉积的去申拉组 (107~100 Ma, 吴浩等, 2013; Xu *et al.*, 2015; Chen *et al.*, 2017) 的出现才代表班怒洋的关闭 (Fan *et al.*, 2014). 同时, 锆石 U-Pb 年代学研究获得代表洋壳存在的洞错蛇绿岩内堆晶橄长岩 (132±3 Ma, Bao *et al.*, 2007)、洞错北仲岗洋岛辉长岩 (116 Ma, Fan *et al.*, 2014)、东巧西塔仁本洋岛玄武岩 (108 Ma, 朱弟成等, 2006b) 和觉翁 (蓬错) 蛇绿岩内堆晶辉长岩 (120 Ma, 陈玉禄等, 2006) 均成岩于早白垩世, 以及在洞错蛇绿岩内发现 131~124 Ma 的放射虫硅质岩 (Baxter *et al.*, 2009), 反映在 132~108 Ma 间班公湖-怒江特提斯洋的东巧-洞错段的洋盆并未完全关闭. 这与

班公湖—怒江洋关闭自东至西具有穿时性,班戈及其以东在 120~117 Ma 关闭,班戈—改则段在 107 Ma 后关闭和改则—日土段在早白垩世晚期—晚白垩世早期(约 100 Ma)关闭的认识相一致(樊帅权等,2010;Fan *et al.*, 2014),也与潘桂棠等(2006)和 Zhang *et al.*(2012)综合班怒缝合带蛇绿岩、岩浆岩和大地构造演化研究得出的班公湖—怒江洋在早白垩世中晚期以后闭合的认识相符。最近,在班公湖—怒江缝合带中西段发现的早白垩世(115~120 Ma)陆缘弧岩浆岩(Li *et al.*, 2017;丁帅等,2017)和晚白垩世早期(85~99 Ma)碰撞造山岩浆岩(Li *et al.*, 2017;张志等,2017;郑有业等,2017)的发现,也进一步佐证了班公湖—怒江洋的中西段在早白垩世中早期尚未关闭。可见,白垩世中早期班公湖—怒江中特提斯洋的班戈—改则段并未完全关闭,拉萨地体北部永珠地区 121~115 Ma 的岩浆活动发生时,其北部的班公湖—怒江洋壳尚处于俯冲消减阶段,锆石 Hf 同位素示踪研究表明,永珠地区早白垩世岩浆岩与拉萨地体中北部及南羌塘南缘由班公湖—怒江洋壳俯冲形成的早白垩世岩浆岩具相似的 $\epsilon_{\text{Hf}}(t)$ -U-Pb 年龄模式(图 10)(Zhu *et al.*, 2011, 2016; Li *et al.*, 2013b, 2014a, 2016; Fan *et al.*, 2015)。因此,本文认为永珠地区早白垩世岩浆岩应该形成于班公湖—怒江特提斯洋壳南向俯冲的大陆边缘弧环境。

综上,认为永珠地区早白垩世岩浆岩形成于班公湖—怒江特提斯洋壳南向俯冲构造背景下的大陆边缘弧环境,也一定程度上反映永珠地区北侧的班公湖—怒江中特提斯洋在 121~115 Ma 期间尚未彻底关闭,仍处于俯冲消减状态。

6.2 岩浆岩成因和源区特征

永珠地区早白垩世火山岩以流纹岩、英安岩、安山岩为主,仅有少量玄武岩;侵入岩为黑云母二长花岗岩和花岗斑岩;中、酸性岩浆岩均属于高钾钙碱性系列,为形成于大陆边缘弧环境的岩浆岩。研究表明岩浆岩的成因有 3 种模式:(1)古老地壳物质部分熔融形成,其锆石 $\epsilon_{\text{Hf}}(t)$ 值低于球粒陨石值;(2)新生地壳物质(火成岩)或地幔物质部分熔融形成,其锆石 $\epsilon_{\text{Hf}}(t)$ 值高于球粒陨石值;(3)壳源岩浆和幔源岩浆混合形成的混合岩浆生成,其锆石 $\epsilon_{\text{Hf}}(t)$ 值在球粒陨石附近变化(Miller, 1985; Le Fort *et al.*, 1987; Alberto and Douce, 1995; Kinny and Maas, 2003; Belousova *et al.*, 2006; Andersen *et al.*, 2007; Ji *et al.*, 2009)。雄梅黑云母二长花岗岩和达

过南流纹岩的锆石 $\epsilon_{\text{Hf}}(t)$ 值分别为 -1.21~3.01 和 -0.68~5.35,在锆石 U-Pb 年龄和 $\epsilon_{\text{Hf}}(t)$ 值图上位于球粒陨石线(CHUR)附近(图 10),与拉萨地体北部由班公湖—怒江中特提斯洋壳俯冲导致幔源物质上涌形成的壳幔混源岩浆岩(130~110 Ma)特征一致(Zhu *et al.*, 2011, 2013, 2016),其对应的 t_{DM2} 分别为 989~1 255 Ma 和 839~1 219 Ma,与拉萨地体北部局部出露的新元古界念青唐古拉群(845~1 250 Ma, Xu *et al.*, 1985; 朱志勇等,2004; 吴勇等,2016)基底地层的年龄基本一致,反映了永珠地区酸性岩浆岩应为有幔源物质参与,并有古老地壳部分熔融物质混入的壳幔混源岩浆成因。

而且,永珠地区的早白垩世岩浆岩以酸性岩(流纹岩和花岗岩类)为主,安山岩和玄武岩出露面积很小(曲永贵等,2003,多巴幅 1:25 万区域地质调查报告;董永胜等,2012,西藏 1:50 000 青卡卡等四幅区域地质调查;刘振宇等,2015,西藏 1:50 000 雄梅镇等四幅区域地质调查报告),因此,由基性岩浆通过结晶分异(Bacon and Druitt, 1988; Wilson, 1993; Mingram *et al.*, 2000; Ingle *et al.*, 2002; Peccerillo, 2003; Bonin, 2004)产生大规模的中酸性岩浆岩显然不可能(Shinjo and Kato, 2000),由幔源岩浆上涌导致下地壳物质部分熔融形成的壳幔混源岩浆(Hildreth and Moorbath, 1988; Roberts and Clemens, 1993; Tepper *et al.*, 1993; Guffanti *et al.*, 1996; Shinjo and Kato, 2000)解释其成因较为合理。研究表明,地壳物质参与形成的花岗岩多为过铝质(Barbarin, 1999),本文黑云母二长花岗岩和花岗斑岩均为过铝质(A/CNK=1.05~1.18),且中一

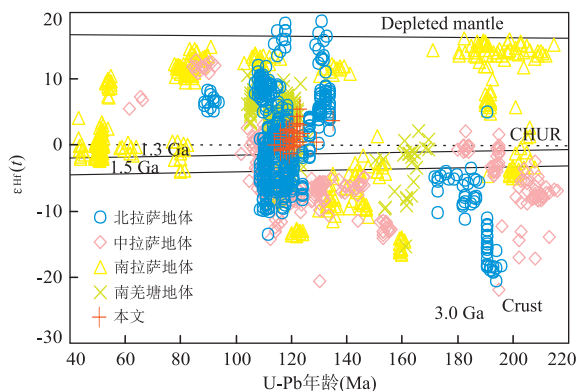


图 10 永珠地区岩浆岩 $\epsilon_{\text{Hf}}(t)$ -U-Pb 年龄

Fig.10 Plots of $\epsilon_{\text{Hf}}(t)$ vs. U-Pb ages diagram for the magmatic rocks of Yongzhu region

北拉萨、中拉萨和南拉萨地体数据引自 Zhu *et al.*(2011, 2016); 南羌塘地体数据引自 Li *et al.*(2013b, 2014a, 2016); Fan *et al.*(2015)

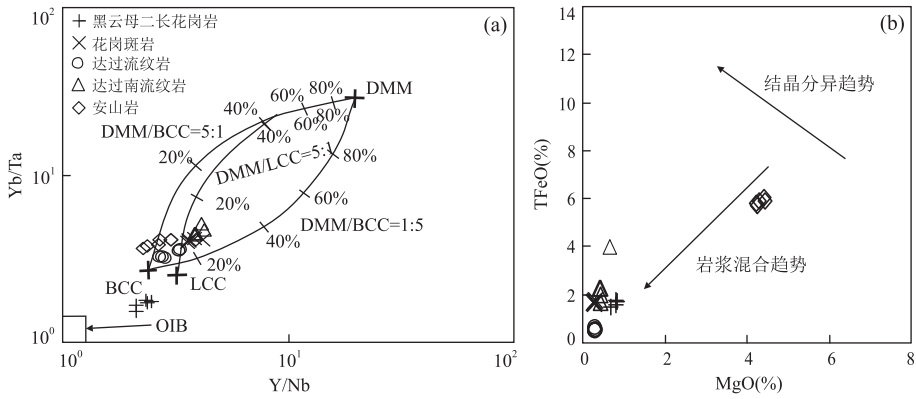


图 11 永珠地区岩浆岩 Yb/Ta-Y/Nb 图解(a)和 TFeO-MgO 成因判别图(b)

Fig.11 Yb/Ta-Y/Nb (a) and TFeO-MgO (b) discrimination diagrams of petrogenesis for magmatic rocks of Yongzhu region
图 a 数据来源: BCC. 平均大陆地壳(Rudnick and Gao, 2003); LCC. 大陆下地壳(Rudnick and Gao, 2003); DMM. 亏损地幔(Salters and Stracke, 2004); 图 b 据 Zorpi *et al.*, 1991

酸性岩浆岩均有较高的 Th 和 LREE 含量, 显示成岩过程中有地壳组分的加入 (Sun *et al.*, 2004; Hanyu *et al.*, 2006); 作为地壳混染指数的 La/Nb 值为 2.08~4.31, 平均 3.16, La/Ta 值为 15.13~55.15, 平均 32.79, 远大于地壳混染可以忽略不计的 $La/Nb \ll 1$ 和 $La/Ta < 22$ 参数 (Fitton *et al.*, 1988; Leat *et al.*, 1988), 亦代表源区有地壳物质的参与; 在 Yb/Ta-Y/Nb 图 (图 11a) 中可见岩浆岩投点均在下地壳和亏损地幔混合线区域并靠近平均地壳, 表明地壳物质在永珠地区早白垩世岩浆岩形成过程中有着重要作用. 下地壳部分熔融形成的岩浆岩的 $Mg^\#$ 一般小于 40 (Atherton and Petford, 1993), 玄武岩部分熔融形成的岩浆岩的 $Mg^\# > 45$ (Rapp, 1997), 有比玄武质更基性物质混入的岩浆 $Mg^\# > 50$ (Wu *et al.*, 2003a, 2003b), 直接由地幔楔橄榄岩部分熔融形成的 $Mg^\# > 60$ (McCarron and Smellie, 1998). 研究区内酸性岩浆岩的 $Mg^\#$ 分布于 13~48 之间, 反映其岩浆不完全来源于壳源物质, 而是有幔源物质的混入; 安山岩的 $Mg^\#$ 值在 57~58 之间, 说明其岩浆以幔源为主, 并受到壳源岩浆的混染 (Zorpi *et al.*, 1991). 这一混源岩浆特征在图 11b 中得到印证.

研究发现, 由角闪岩相俯冲大洋板片脱水熔融参与形成的岩浆岩具有: (1) 多为酸性岩, 并出现少量安山岩; (2) 不出现石榴子石; (3) 具壳-幔混源岩浆的同位素特征; (4) 具弧岩浆岩的地球化学特征; (5) Nb/Ta 比值低于球粒陨石的 Nb/Ta 比值; (6) 不含较高的 Sr (Mo *et al.*, 2008). 永珠地区早白垩世岩浆岩以酸性岩为主, 并有部分安山岩, 无石榴子石出现, Hf 同位素为壳幔混源岩浆特征, 地球化学

显示弧岩浆岩的特征, Nb/Ta 比值 (6.5~13.8) 低于球粒陨石的 Nb/Ta 比值 (~17.6, Sun and MacDonough, 1989), Sr 含量也不高 (表 1, 图 5), 这在一定程度上表明永珠地区早白垩世岩浆岩的形成可能与班公湖-怒江洋壳的俯冲板片的脱水熔融有关.

前文讨论了永珠地区早白垩世岩浆岩的地球化学和 Hf 同位素均显示具壳幔混源特征, 考虑其成岩期间处于班公湖-怒江洋壳南向俯冲的大陆边缘弧环境, 推测俯冲的班公湖-怒江洋壳板片由于板块间摩擦及高温地幔热传递, 加之上覆岩石的静压力, 俯冲到一定深度会发生角闪岩-榴辉岩等不同程度相变 (Defant and Drummond, 1990), 进而洋壳含水矿物脱水促使板片发生部分熔融上涌, 高温熔体诱发地幔楔部分熔融, 产生亏损重稀土和 Nb、Ta 等高场强元素、富集轻稀土和大离子亲石元素的弧岩浆 (White and Patchett, 1984), 并在上侵过程中遭受下地壳念青唐古拉群角闪岩相地层 (朱志勇等, 2004; 吴勇等, 2016) 不同程度的混染和经历熔融、同化、存储、均一过程 (Hildreth and Moorbath, 1988; Taylor and McLennan, 1995), 进而在地壳浅部形成岩浆房. 永珠地区早白垩世岩浆岩具有微量元素 Ba、Sr 和 Eu 亏损 (图 5b, 5d), 表明其源区存在钾长石和斜长石的结晶残留 (Patino and Johnston, 1991; Wu *et al.*, 2003a, 2003b). 岩浆岩的 Nb、Ta 亏损, 而 Y 不显示异常, 指示岩浆源区有石榴子石或角闪石残留 (Pearce and Mei, 1988); 根据 HREE 元素在石榴子石和角闪石中分配系数的差异, 可识别出 HREE 为倾斜模式和 Y/Yb 比值明显大于 10 时, 源区主要残留石榴子石; HREE 为较平坦配分模式和 Y/Yb 小于 10 时, 源区主要残留角闪石

(Sisson, 1994; 高永丰等, 2003), 本文岩浆岩明显为 Nb、Ta 亏损而 Y 无异常, HREE 较为平坦(图 5b, 5d), 且 Y/Yb 比值为 8.2~9.9 之间, 表明源区残留有角闪石。上述表明, 形成永珠地区早白垩世岩浆岩的岩浆源区残留有斜长石、钾长石和角闪岩。

综上, 笔者认为永珠地区早白垩世岩浆岩为班公湖—怒江中特提斯洋壳俯冲消减过程中上涌的幔源物质与下地壳角闪岩相物质混溶的产物, 其岩浆应由俯冲的班公湖—怒江中特提斯洋板片在深部脱水熔融, 进而诱发上覆地幔楔部分熔融形成基性岩浆上涌, 导致下地壳物质发生部分熔融形成酸性岩浆, 它们在上升过程中按不同比例混合形成中性和酸性岩浆, 并侵入到地下或喷出地表形成侵入岩和火山岩。

7 结论

(1) 获得永珠地区黑云母二长花岗岩的锆石 U-Pb 年龄为 118 ± 1.0 Ma, 流纹岩的锆石 U-Pb 年龄为 121 ± 0.8 Ma, 安山岩的锆石 U-Pb 年龄为 115 ± 0.8 Ma, 均成岩于早白垩世。

(2) 永珠地区早白垩世岩浆岩以酸性岩为主, 属于高钾钙碱性系列, 亏损高场强元素 Nb、Ta、P、Ti 和大离子亲石元素 Ba、Sr, 富集大离子亲石元素 Rb、K 和放射性元素 U、Th, 为大陆边缘弧岩浆岩特征; 岩石地球化学和 Lu-Hf 同位素显示它们均为壳幔混源岩浆岩, 且源区有角闪石、钾长石和斜长石残留。

(3) 结合拉萨地体的演化过程, 认为永珠地区早白垩世岩浆岩形成于班公湖—怒江特提斯洋壳南向俯冲作用下的大陆边缘弧环境, 由俯冲的班公湖—怒江中特提斯洋板片在深部脱水熔融, 进而诱发上覆地幔楔部分熔融形成的基性岩浆上涌, 导致下地壳物质发生部分熔融形成酸性岩浆, 它们在上升过程中按不同比例混合, 形成中性和酸性岩浆侵入到地下或喷出地表, 形成侵入岩和火山岩。

致谢: 胡兆初教授、罗涛博士在 LA-ICP-MS 锆石 U-Pb 测年过程中的大力帮助, 匿名专家提出了宝贵的修改意见, 在此一并感谢!

References

Aitchison, J. C., Ali, J. R., Davis, A. M., 2007. When and Where did India and Asia Collide? *Journal of Geophysical Research*, 112 (B5): 51–70. <https://doi.org/10.1029/2006JB004706>

- Alberto, E., Douce, P., 1995. Experimental Generation of Hybrid Silicic Melts by Reaction of High-Al Basalt with Metamorphic Rocks. *Journal of Geophysical Research: Solid Earth*, 100 (B8): 15623–15639. <https://doi.org/10.1029/94jb03376>
- Andersen, T., Griffin, W. L., Sylvester, A. G., 2007. Sveconorwegian Crustal Underplating in Southwestern Fennoscandia: LAM-ICPMS U-Pb and Lu-Hf Isotope Evidence from Granites and Gneisses in Telemark, Southern Norway. *Lithos*, 93 (3–4): 273–287. <https://doi.org/10.1016/j.lithos.2006.03.068>
- Atherton, M. P., Petford, N., 1993. Generation of Sodium-Rich Magmas from Newly Underplated Basaltic Crust. *Nature*, 362 (6416): 144–146. <https://doi.org/10.1038/362144a0>
- Bacon, C. R., Druitt, T. H., 1988. Compositional Evolution of the Zoned Calcalkaline Magma Chamber of Mount Mazama, Crater Lake, Oregon. *Contributions to Mineralogy and Petrology*, 98 (2): 224–256. <https://doi.org/10.1007/bf00402114>
- Bao, P. S., Xiao, X. C., Su, L., et al., 2007. Geochemical Characteristics and Isotopic Dating for the Dongcuo Ophiolite, Tibet Plateau. *Science China Earth Sciences*, 50 (5): 660–671.
- Barbarin, B., 1999. A Review of the Relationships between Granitoid Types, Their Origins and Their Geodynamic Environments. *Lithos*, 46 (3): 605–626. [https://doi.org/10.1016/s0024-4937\(98\)00085-1](https://doi.org/10.1016/s0024-4937(98)00085-1)
- Baxter, A. T., Aitchison, J. C., Zyabrev, S. V., 2009. Radiolarian Age Constraints on Mesotethyan Ocean Evolution, and Their Implications for Development of the Bangong-Nujiang Suture, Tibet. *Journal of the Geological Society*, 166 (4): 689–694. <https://doi.org/10.1144/0016-76492008-128>
- Belousova, E. A., Griffin, W. L., O'Reilly, S. Y., 2006. Zircon Crystal Morphology, Trace Element Signatures and Hf Isotope Composition as a Tool for Petrogenetic Modelling: Examples from Eastern Australian Granitoids. *Journal of Petrology*, 47 (2): 329–353. <https://doi.org/10.1093/ptrology/egi077>
- Bonin, B., 2004. Do Coeval Mafic and Felsic Magmas in Post-Collisional to Within-Plate Regimes Necessarily Imply Two Contrasting, Mantle and Crustal, Sources? A Review. *Lithos*, 78 (1–2): 1–24. <https://doi.org/10.1016/j.lithos.2004.04.042>
- Bouvier, A., Vervoort, J. D., Patchett, P. J., 2008. The Lu-Hf and Sm-Nd Isotopic Composition of CHUR: Constraints

- from Unequilibrated Chondrites and Implications for the Bulk Composition of Terrestrial Planets, *Earth and Planetary Science Letters*, 273(1-2): 48-57. <https://doi.org/10.1016/j.epsl.2008.06.010>
- Chen, W. W., Yang, T. S., Zhang, S. H., et al., 2012. Paleomagnetic Results from the Early Cretaceous Zenong Group Volcanic Rocks, Cuoqin, Tibet, and Their Paleogeographic Implications. *Gondwana Research*, 22(2): 461-469. <https://doi.org/10.1016/j.gr.2011.07.019>
- Chen, W. W., Zhang, S. H., Ding, J. K., et al., 2017. Combined Paleomagnetic and Geochronological Study on Cretaceous Strata of the Qiangtang Terrane, Central Tibet. *Gondwana Research*, 41: 373-389. <https://doi.org/10.1016/j.gr.2015.07.004>
- Chen, Y., Zhu, D. C., Zhao, Z. D., et al., 2014. Slab Break off Triggered ca. 113 Ma Magmatism around Xainza Area of the Lhasa Terrane, Tibet. *Gondwana Research*, 26(2): 449-463. <https://doi.org/10.1016/j.gr.2013.06.005>
- Chen, G. R., Liu, H. F., Jiang, G. W., et al., 2004. Discovery of the Shamuluo Formation in the Central Segment of the Bangong Co-Nujiang River Suture Zone, Tibet. *Geological Bulletin of China*, 23(2): 193-194 (in Chinese with English abstract).
- Chen, Y., Zhu, D. C., Zhao, Z. D., et al., 2010. Geochronology, Geochemistry and Petrogenesis of the Bamco Andesites from the Northern Gangdese, Tibet. *Acta Petrologica Sinica*, 26(7): 2193-2206 (in Chinese with English abstract).
- Chen, Y. L., Zhang, K. Z., Yang, Z. M., et al., 2006. Discovery of a Complete Ophiolite Section in the Jueweng Area, Nagqu County, in the Central Segment of the Bangong Co-Nujiang Junction Zone, Qinghai-Tibet Plateau. *Geological Bulletin of China*, 25(6): 694-699 (in Chinese with English abstract).
- Chiu, H. Y., Chung, S. L., Wu, F. Y., et al., 2009. Zircon U-Pb and Hf Isotopic Constraints from Eastern Transhimalayan Batholiths on the Precollisional Magmatic and Tectonic Evolution in Southern Tibet. *Tectonophysics*, 477(1-2): 3-19. <https://doi.org/10.1016/j.tecto.2009.02.034>
- Chu, M. F., Chung, S. L., O'Reilly, S. Y., et al., 2011. India's Hidden Inputs to Tibetan Orogeny Revealed by Hf Isotopes of Transhimalayan Zircons and Host Rocks. *Earth and Planetary Science Letters*, 307(3-4): 479-486. <https://doi.org/10.1016/j.epsl.2011.05.020>
- Chu, M. F., Chung, S. L., Song, B., et al., 2006. Zircon U-Pb and Hf Isotope Constraints on the Mesozoic Tectonics and Crustal Evolution of Southern Tibet. *Geology*, 34(9): 745-748. <https://doi.org/10.1130/g22725.1>
- Copeland, P., Harrison, T. M., Pan, Y., et al., 1995. Thermal Evolution of the Gangdese Batholith, Southern Tibet: A History of Episodic Unroofing. *Tectonics*, 14(2): 223-236. <https://doi.org/10.1029/94tc01676>
- Corfu, F., Hanchar, J. M., Hoskin, P. W. O., et al., 2003. Atlas of Zircon Textures. *Reviews in Mineralogy and Geochemistry*, 53(1): 469-500. <https://doi.org/10.2113/0530469>
- Coulon, C., Maluski, H., Bollinger, C., et al., 1986. Mesozoic and Cenozoic Volcanic Rocks from Central and Southern Tibet: ^{39}Ar - ^{40}Ar Dating, Petrological Characteristics and Geodynamical Significance. *Earth and Planetary Science Letters*, 79(3-4): 281-302. [https://doi.org/10.1016/0012-821x\(86\)90186-x](https://doi.org/10.1016/0012-821x(86)90186-x)
- Crosson, R. S., Owens, T. J., 1987. Slab Geometry of the Cascadia Subduction Zone beneath Washington from Earthquake Hypocenters and Teleseismic Converted Waves (USA). *Geophysical Research Letters*, 14(8): 824-827. <https://doi.org/10.1029/GL014i008p00824>
- DeCelles, P. G., Kapp, P., Ding, L., et al., 2007. Late Cretaceous to Middle Tertiary Basin Evolution in the Central Tibetan Plateau: Changing Environments in Response to Tectonic Partitioning, Aridification, and Regional Elevation Gain. *Geological Society of America Bulletin*, 119(5-6): 654-680. <https://doi.org/10.1130/b26074.1>
- Defant, M. J., Drummond, M. S., 1990. Derivation of Some Modern Arc Magmas by Melting of Young Subducted Lithosphere. *Nature*, 347(6294): 662-665. <https://doi.org/10.1038/347662a0>
- Deng, J. F., Xiao, Q. H., Su, S. G., et al., 2007. Igneous Petrotectonic Assemblages and Tectonic Settings: A Discussion. *Geological Journal of China Universities*, 13(3): 392-402 (in Chinese with English abstract).
- Ding, L., Kapp, P., Yin, A., et al., 2003. Early Tertiary Volcanism in the Qiangtang Terrane of Central Tibet: Evidence for a Transition from Oceanic to Continental Subduction. *Journal of Petrology*, 44: 1833-1865.
- Ding, L., Zhao, Y. Y., Yang, Y. Q., et al., 2012. LA-ICP-MS Zircon U-Pb Dating and Geochemical Characteristics of Ore-Bearing Granite in Skarn-Type Iron Polymetallic Deposits of Duoba Area, Baingoin County, Tibet, and Their Significance. *Acta Petrologica et Mineralogica*, 31(4): 479-496 (in Chinese with English abstract).
- Ding, S., Tang, J. X., Zheng, W. B., et al., 2017. Geochronology and Geochemistry of Naruo Porphyry Cu(Au) Deposit in Duolong Ore-Concentrated Area, Tibet, and Their Geological Significance. *Earth Science*, 42(1): 1-23 (in Chinese with English abstract).
- Dong, X., Zhang, Z. M., Santosh, M., 2010. Zircon U-Pb Chro-

- nology of the Nyingtri Group, Southern Lhasa Terrane, Tibetan Plateau: Implications for Grenvillian and Pan-African Provenance and Mesozoic-Cenozoic Metamorphism. *The Journal of Geology*, 118 (6): 677 – 690. <https://doi.org/10.1086/656355>
- Fan, J. J., Li, C., Xie C. M., et al., 2014. Petrology, Geochemistry, and Geochronology of the Zhonggang Ocean Island, Northern Tibet: Implications for the Evolution of the Banggongco-Nujiang Oceanic Arm of the Neo-Tethys. *International Geology Review*, 56 (12): 1504 – 1520. <https://doi.org/10.1080/00206814.2014.947639>
- Fan, J. J., Li, C., Xie, C. M., et al., 2015. Petrology and U-Pb Zircon Geochronology of Bimodal Volcanic Rocks from the Maierze Group, Northern Tibet: Constraints on the Timing of Closure of the Banggong-Nujiang Ocean. *Lithos*, 227: 148 – 160. <https://doi.org/10.1016/j.lithos.2015.03.021>
- Fan, S. Q., Shi, R. D., Ding, L., et al., 2010. Geochemical Characteristics and Zircon U-Pb Age of the Plagiogranite in Gaize Ophiolite of Central Tibet and Their Tectonic Significance. *Acta Petrologica et Mineralogica*, 29 (5): 467 – 478 (in Chinese with English abstract).
- Fitton, J. G., James, D., Kempton, P. D., et al., 1988. The Role of Lithospheric Mantle in the Generation of Late Cenozoic Basic Magmas in the Western United States. *Journal of Petrology, Special Volume*, (1): 331 – 349. https://doi.org/10.1093/petrology/special_volume.1.331
- Gao, S. B., Zheng, Y. Y., Wang, J. S., et al., 2011a. The Geochronology and Geochemistry of Intrusive Rocks in Bange Area: Constraints on the Evolution Time of the Bangong Lake-Nujiang Ocean Basin. *Acta Petrologica Sinica*, 27 (7): 1973 – 1982 (in Chinese with English abstract).
- Gao, S. B., Zheng, Y. Y., Xie, M. C., et al., 2011b. Geodynamic Setting and Mineralizational Implication of the Xueru Intrusion in Ban'ge, Tibet. *Earth Science*, 36 (4): 729 – 739 (in Chinese with English abstract).
- Gao, Y. F., Hou, Z. Q., Wei, R. H., 2003. Neogene Porphyries from Gangdese: Petrological, Geochemical Characteristics and Geodynamic Significances. *Acta Petrologica Sinica*, 19 (3): 418 – 428 (in Chinese with English abstract).
- Geng, Q. R., Mao, X. C., Zhang, Z., et al., 2015. New Understanding in the Middle and West Part of Bangong Lake-Nujiang River Metallogenic Belt and Its Implication for Prospecting. *Geological Survey of China*, 2 (2): 1 – 11 (in Chinese with English abstract).
- Geng, Q. R., Pan, G. T., Wang, L. Q., et al., 2011. Tethyan Evolution and Metallogenic Geological Background of the Bangong Co-Nujiang Belt and the Qiangtang Massif in Tibet. *Geological Bulletin of China*, 30 (8): 1261 – 1274 (in Chinese with English abstract).
- Gorton, M. P., Schandl, E. S., 2000. From Continents to Island Arcs: A Geochemical Index of Tectonic Setting for Arc-Related and Within-Plate Felsic to Intermediate Volcanic Rocks. *The Canadian Mineralogist*, 38 (5): 1065 – 1073. <https://doi.org/10.2113/gscanmin.38.5.1065>
- Griffin, W. L., Pearson, N. J., Belousova, E., et al., 2000. The Hf Isotope Composition of Cratonic Mantle: LAM-MC-ICP MS Analysis of Zircon Megacrysts in Kimberlites. *Geochimica et Cosmochimica Acta*, 64 (1): 133 – 147. [https://doi.org/10.1016/s0016-7037\(99\)00343-9](https://doi.org/10.1016/s0016-7037(99)00343-9)
- Guan, J. L., Geng, Q. R., Wang, G. Z., et al., 2014. Geochemical, Zircon U-Pb Dating and Hf Isotope Compositions Studies of the Granite in Ritu County-Lameila Pass Area, North Gangdese, Tibet. *Acta Petrologica Sinica*, 30 (6): 1666 – 1684 (in Chinese with English abstract).
- Guffanti, M., Clynnne, M. A., Muffler, L. J. P., 1996. Thermal and Mass Implications of Magmatic Evolution in the Lassen Volcanic Region, California, and Minimum Constraints on Basalt Influx to the Lower Crust. *Journal of Geophysical Research: Solid Earth*, 101 (B2): 3003 – 3013. <https://doi.org/10.1029/95jb03463>
- Gutscher, M. A., Maury, R., Eissen, J. P., et al., 2000. Can Slab Melting be Caused by Flat Subduction? *Geology*, 28 (6): 535 – 538. [https://doi.org/10.1130/0091-7613\(2000\)028<0535:csmbcb>2.3.co;2](https://doi.org/10.1130/0091-7613(2000)028<0535:csmbcb>2.3.co;2)
- Hall, A., 1989. Igneous Petrogenesis: A Global Tectonic Approach. *Mineralogical Magazine*, 53 (372): 514 – 515. <https://doi.org/10.1180/minmag.1989.053.372.15>
- Hanyu, T., Tatsumi, Y., Nakai, S., et al., 2006. Contribution of Slab Melting and Slab Dehydration to Magmatism in the NE Japan Arc for the Last 25 Myr: Constraints from Geochemistry. *Geochemistry, Geophysics, Geosystems*, 7 (8): 1 – 29. <https://doi.org/10.1029/2005gc001220>
- Hao, L. L., Wang, Q., Wyman, D. A., et al., 2016. Underplating of Basaltic Magmas and Crustal Growth in a Continental Arc: Evidence from Late Mesozoic Intermediate-Felsic Intrusive Rocks in Southern Qiangtang, Central Tibet. *Lithos*, 245: 223 – 242. <https://doi.org/10.1016/j.lithos.2015.09.015>
- Harris, N., Massey, J., 1994. Decompression and Anatexis of Himalayan Metapelites. *Tectonics*, 13 (6): 1537 – 1546. <https://doi.org/10.1029/94tc01611>
- Hildreth, W., Moorbath, S., 1988. Crustal Contributions to Arc Magmatism in the Andes of Central Chile. *Contributions to Mineralogy and Petrology*, 98 (4): 455 – 489.

<https://doi.org/10.1007/bf00372365>

- Hoskin, P. W. O., Schaltegger, U., 2003. The Composition of Zircon and Igneous and Metamorphic Petrogenesis. *Reviews in Mineralogy and Geochemistry*, 53(1): 27–62. <https://doi.org/10.2113/0530027>
- Hou, K. J., Li, Y. H., Zou, T. R., et al., 2007. Laser Ablation-MC-ICP-MS Technique for Hf Isotope Microanalysis of Zircon and Its Geological Applications. *Acta Petrologica Sinica*, 23(10): 2595–2604 (in Chinese with English abstract).
- Hu, J., Wan, Y. W., Tao, Z., et al., 2014. New Geochemistry and Geochronology Evidences Related to Southward Subduction of Tethys Ocean Basin in West Segment of Bangonghu-Nujiang Suture Belt. *Journal of Chengdu University of Technology (Science & Technology Edition)*, 41(4): 505–515 (in Chinese with English abstract).
- Hu, Z. C., Liu, Y. S., Gao, S., et al., 2012. Improved In Situ Hf Isotope Ratio Analysis of Zircon Using Newly Designed X Skimmer Cone and Jet Sample Cone in Combination with the Addition of Nitrogen by Laser Ablation Multiple Collector ICP-MS. *Journal of Analytical Atomic Spectrometry*, 27(9): 1391–1399. <https://doi.org/10.1039/c2ja30078h>
- Huang, H. X., Li, G. M., Dong, S. L., et al., 2012. SHRIMP Zircon U-Pb Age and Geochemical Characteristics of Qinglung Granodiorite in Baingoin Area, Tibet. *Geological Bulletin of China*, 31(6): 852–859 (in Chinese with English abstract).
- Huang, Y., Zhu, D. C., Zhao, Z. D., et al., 2012. Petrogenesis and Implication of the Andesites at ~113 Ma in the Nagqu Region in the Northern Lhasa Subterranean. *Acta Petrologica Sinica*, 28(5): 1603–1614 (in Chinese with English abstract).
- Ingle, S., Weis, D., Frey, F. A., 2002. Indian Continental Crust Recovered from Elan Bank, Kerguelen Plateau (ODP Leg 183, Site 1137). *Journal of Petrology*, 43(7): 1241–1257. <https://doi.org/10.1093/petrology/43.7.1241>
- Ji W. Q., Wu, F. Y., Chung, S. L., et al., 2009. Zircon U-Pb Geochronology and Hf Isotopic Constraints on Petrogenesis of the Gangdese Batholith, Southern Tibet. *Chemical Geology*, 262(3–4): 229–245. <https://doi.org/10.1016/j.chemgeo.2009.01.020>
- Kang, L., Xiao, P. X., Gao, X. F., et al., 2012. The Age and Origin of the Konjirap Pluton in Northwestern Tibetan Plateau and Its Tectonic Significances. *Acta Geologica Sinica*, 86(7): 1063–1076 (in Chinese with English abstract).
- Kang, Z. Q., Xu, J. F., Wang, B. D., et al., 2009. Geochemistry of Cretaceous Volcanic Rocks of Duoni Formation in Northern Lhasa Block: Discussion of Tectonic Setting. *Earth Science*, 34(1): 89–104 (in Chinese with English abstract).
- Kapp, P., DeCelles, P. G., Gehrels, G. E., et al., 2007. Geological Records of the Lhasa-Qiangtang and Indo-Asian Collisions in the Nima Area of Central Tibet. *Geological Society of America Bulletin*, 119(7–8): 917–933. <https://doi.org/10.1130/b26033.1>
- Kapp, P., Murphy, M. A., Yin, A., et al., 2003. Mesozoic and Cenozoic Tectonic Evolution of the Shiquanhe Area of Western Tibet. *Tectonics*, 22(4): 3–1–3–24. <https://doi.org/10.1029/2001tc001332>
- Kinny, P. D., Maas, R., 2003. Lu-Hf and Sm-Nd Isotope Systems in Zircon. *Reviews in Mineralogy and Geochemistry*, 53(1): 327–341. <https://doi.org/10.2133/0530327>
- Le Fort, P., Cuney, M., Deniel, C., et al., 1987. Crustal Generation of the Himalayan Leucogranites. *Tectonophysics*, 134(1–3): 39–57. [https://doi.org/10.1016/0040-1951\(87\)90248-4](https://doi.org/10.1016/0040-1951(87)90248-4)
- Leat, P. T., Thompson, R. N., Morrison, M. A., et al., 1988. Compositionally-Diverse Miocene-Recent Rift-Related Magmatism in Northwest Colorado: Partial Melting, and Mixing of Mafic Magmas from 3 Different Asthenospheric and Lithospheric Mantle Sources. *Journal of Petrology, Special Volume*, (1): 351–377. https://doi.org/10.1093/petrology/special_volume.1.351
- Leier, A. L., DeCelles, P. G., Kapp, P., et al., 2007. Lower Cretaceous Strata in the Lhasa Terrane, Tibet, with Implications for Understanding the Early Tectonic History of the Tibetan Plateau. *Journal of Sedimentary Research*, 77(10): 809–825. <https://doi.org/10.2110/jsr.2007.078>
- Li, G. M., Qin, K. Z., Li, J. X., et al., 2017. Cretaceous Magmatism and Metallogeny in the Bangong-Nujiang Metamorphic Belt, Central Tibet: Evidence from Petrogeochemistry, Zircon U-Pb Ages, and Hf-O Isotopic Compositions. *Gondwana Research*, 41: 110–127. <https://doi.org/10.1016/j.gr.2015.09.006>
- Li, J. F., Xia, B., Xia, L. Z., et al., 2013a. Geochronology of the Dong Tso Ophiolite and the Tectonic Environment. *Acta Geologica Sinica (English Edition)*, 87(6): 1604–1616. <https://doi.org/10.1111/1755-6724.12162>
- Li, J. X., Qin, K. Z., Li, G. M., et al., 2013b. Petrogenesis of Ore-Bearing Porphyries from the Duolong Porphyry Cu-Au Deposit, Central Tibet: Evidence from U-Pb Geochronology, Petrochemistry and Sr-Nd-Hf-O Isotope Characteristics. *Lithos*, 160–161: 216–227. <https://doi.org/10.1016/j.lithos.2012.12.015>
- Li, J. X., Qin, K. Z., Li, G. M., et al., 2014a. Geochronology, Geochemistry, and Zircon Hf Isotopic Compositions of Mesozoic Intermediate-Felsic Intrusions in Central Tibet: Petroge-

- netic and Tectonic Implications. *Lithos*, 198—199: 77—91. <https://doi.org/10.1016/j.lithos.2014.03.025>
- Li, J. X., Qin, K. Z., Li, G. M., et al., 2016. Petrogenesis of Cretaceous Igneous Rocks from the Duolong Porphyry Cu-Au Deposit, Central Tibet: Evidence from Zircon U-Pb Geochronology, Petrochemistry and Sr-Nd-Pb-Hf Isotope Characteristics. *Geological Journal*, 51(2): 285—307. <https://doi.org/10.1002/gj.2631>
- Li, S. M., Zhu, D. C., Wang, Q., et al., 2014b. Northward Subduction of Bangong-Nujiang Tethys: Insight from Late Jurassic Intrusive Rocks from Bangong Tso in Western Tibet. *Lithos*, 205: 284—297. <https://doi.org/10.1016/j.lithos.2014.07.010>
- Li, Z. Y., Ding, L., Song, P. P., et al., 2017. Paleomagnetic Constraints on the Paleolatitude of the Lhasa Block during the Early Cretaceous: Implications for the Onset of India-Asia Collision and Latitudinal Shortening Estimates across Tibet and Stable Asia. *Gondwana Research*, 41: 352—372. <https://doi.org/10.1016/j.gr.2015.05.013>
- Li, C., Zhai, G. Y., Wang, L. Q., et al., 2009. An Important Window for Understanding the Qinghai-Tibet Plateau—A Review on Research Progress in Recent Years of Qiangtang Area, Tibet, China. *Geological Bulletin of China*, 28(9): 1169—1177 (in Chinese with English abstract).
- Li, X. B., Wang, B. D., Liu, H., et al., 2015. The Late Jurassic High-Mg Andesites in the Daru Tso Area, Tibet: Evidence for the Subduction of the Bangong Co-Nujiang River Oceanic Lithosphere. *Geological Bulletin of China*, 34(2—3): 251—261 (in Chinese with English abstract).
- Liu, Y. S., Hu, Z. C., Zong, K. Q., et al., 2010. Reappraisal and Refinement of Zircon U-Pb Isotope and Trace Element Analyses by LA-ICP-MS. *Chinese Science Bulletin*, 55(15): 1535—1546. <https://doi.org/10.1007/s11434-010-3052-4>
- Ludwig, K. R., 2003. User's Manual for Isoplot 3.00: A Geochronological Toolkit for Microsoft Excel. *Geochronology Center, Special Publication, Berkeley*, 4: 1—43.
- Maniar, P. D., Piccoli, P. M., 1989. Tectonic Discrimination of Granitoids. *Geological Society of America Bulletin*, 101(5): 635—643. [https://doi.org/10.1130/0016-7606\(1989\)101<0635:tdog>2.3.co;2](https://doi.org/10.1130/0016-7606(1989)101<0635:tdog>2.3.co;2)
- McCarron, J. J., Smellie, J. L., 1998. Tectonic Implications of Fore-Arc Magmatism and Generation of High-Magnesian Andesites: Alexander Island, Antarctica. *Journal of the Geological Society*, 155(2): 269—280. <https://doi.org/10.1144/gsjgs.155.2.0269>
- McCulloch, M. T., Gamble, J. A., 1991. Geochemical and Geodynamical Constraints on Subduction Zone Magmatism. *Earth and Planetary Science Letters*, 102(3—4): 358—374. [https://doi.org/10.1016/0012-821x\(91\)90029-h](https://doi.org/10.1016/0012-821x(91)90029-h)
- Metcalf, I., 2013. Gondwana Dispersion and Asian Accretion: Tectonic and Palaeogeographic Evolution of Eastern Tethys. *Journal of Asian Earth Sciences*, 66: 1—33. <https://doi.org/10.1016/j.jseae.2012.12.020>
- Metcalf, I., 1998. Palaeozoic and Mesozoic Geological Evolution of the SE Asian Region: Multidisciplinary Constraints and Implications for Biogeography. In: Hall, R., Holloway, J. D., eds., *Biogeography and Geological Evolution of SE Asia*. Backhuys Publishers, Amsterdam, 25—41.
- Miller, C. F., 1985. Are Strongly Peraluminous Magmas Derived from Pelitic Sedimentary Sources? *The Journal of Geology*, 93(6): 673—689. <https://doi.org/10.1086/628995>
- Miller, C., Schuster, R., Kiötzi, U., et al., 1999. Post-Collisional Potassic and Ultrapotassic Magmatism in SW Tibet: Geochemical and Sr-Nd-Pb-O Isotopic Constraints for Mantle Source Characteristics and Petrogenesis. *Journal of Petrology*, 40(9): 1399—1424. <https://doi.org/10.1093/ptroj/40.9.1399>
- Mingram, B., Trumbull, R. B., Littman, S., et al., 2000. A Petrogenetic Study of Anorogenic Felsic Magmatism in the Cretaceous Paresis Ring Complex, Namibia: Evidence for Mixing of Crust and Mantle-Derived Components. *Lithos*, 54(1—2): 1—22. [https://doi.org/10.1016/s0024-4937\(00\)00033-5](https://doi.org/10.1016/s0024-4937(00)00033-5)
- Miyashiro, A., 1974. Volcanic Rock Series in Island Arcs and Active Continental Margins. *American Journal of Science*, 274(4): 321—355. <https://doi.org/10.2475/ajs.274.4.321>
- Mo, X. X., Hou, Z. Q., Niu, Y. L., et al., 2007. Mantle Contributions to Crustal Thickening during Continental Collision: Evidence from Cenozoic Igneous Rocks in Southern Tibet. *Lithos*, 96(1—2): 225—242. <https://doi.org/10.1016/j.lithos.2006.10.005>
- Mo, X. X., Dong, G. C., Zhao, Z. D., et al., 2005. Spatial and Temporal Distribution and Characteristics of Granitoids in the Gangdese, Tibet and Implication for Crustal Growth and Evolution. *Geological Journal of China Universities*, 11(3): 281—290 (in Chinese with English abstract).
- Mo, X. X., Niu, Y. L., Dong, G. C., et al., 2008. Contribution of Syncollisional Felsic Magmatism to Continental Crust Growth: A Case Study of the Paleocene Linzizong Volcanic Succession in Southern Tibet. *Chemical Geology*, 250: 49—67.
- Mo, X. X., Pan, G. T., 2006. From the Tethys to the Formation of the Qinghai-Tibet Plateau: Constrained by Tectono-Magmatic Events. *Earth Science Frontiers*, 13(6): 43—51 (in Chinese with English abstract).

- Mo, X. X., Zhao, Z. D., Deng, J. F., et al., 2003. Response of Volcanism to the India-Asia Collision. *Earth Science Frontiers*, 10(3): 135—148 (in Chinese with English abstract).
- Muller, D., Groves, D. I., 1994. Potassic Igneous Rocks and Associated Gold-Copper Mineralization. *Lithos*, 56(2): 265—266.
- Murphy, M. A., Yin, A., Harrison, T. M., et al., 1997. Did the Indo-Asian Collision alone Create the Tibetan Plateau? *Geology*, 25(8): 719. [https://doi.org/10.1130/0091-7613\(1997\)025<0719:dtiaca>2.3.co;2](https://doi.org/10.1130/0091-7613(1997)025<0719:dtiaca>2.3.co;2)
- Najman, Y., Appel, E., Boudagher-Fadel, M., et al., 2010. Timing of India-Asia Collision: Geological, Biostratigraphic, and Palaeomagnetic Constraints. *Journal of Geophysical Research*, 115(B12): 1—70. <https://doi.org/10.1029/2010jb007673>
- Niu, Y. L., O'Hara, M. J., Pearce, J. A., 2003. Initiation of Subduction Zones as a Consequence of Lateral Compositional Buoyancy Contrast within the Lithosphere: A Petrological Perspective. *Journal of Petrology*, 44(5): 851—866. <https://doi.org/10.1093/petrology/44.5.851>
- Pan, G. T., Mo, X. X., Hou, Z. Q., et al., 2006. Spatial-Temporal Framework of the Gangdese Orogenic Belt and Its Evolution. *Acta Petrologica Sinica*, 22(3): 521—533 (in Chinese with English abstract).
- Pan, G. T., Wang, L. Q., Li, R. S., et al., 2012. Tectonic Evolution of the Qinghai-Tibet Plateau. *Journal of Asian Earth Sciences*, 53: 3—14. <https://doi.org/10.1016/j.jseaes.2011.12.018>
- Pan, G. T., Zhu, D. C., Wang, L. Q., et al., 2004. Bangong Lake-Nu River Suture Zone—The Northern Boundary of Gondwanaland: Evidence from Geology and Geophysics. *Earth Science Frontiers*, 11(4): 372—382 (in Chinese with English abstract).
- Patino, D. A. E., Johnston, A. D., 1991. Phase Equilibria and Melt Productivity in the Pelitic System: Implications for the Origin of Peraluminous Granitoids and Aluminous Granulites. *Contributions to Mineralogy and Petrology*, 107(2): 202—218. <https://doi.org/10.1007/bf00310707>
- Pearce, J. A., Harris, N. B. W., Tindle, A. G., 1984. Trace Element Discrimination Diagrams for the Tectonic Interpretation of Granitic Rocks. *Journal of Petrology*, 25(4): 956—983. <https://doi.org/10.1093/petrology/25.4.956>
- Pearce, J. A., Mei, H. J., 1988. Volcanic Rocks of the 1985 Tibet Geotraverse: Lhasa to Golmud. *Philosophical Transactions of the Royal Society A: Mathematical, Physical and Engineering Sciences*, 327(1594): 169—201. <https://doi.org/10.1098/rsta.1988.0125>
- Pearce, J. A., 1982. Trace Element Characteristics of Lavas from Destructive Plate Boundaries. *Andesites: Orogenic Andesites and Related Rocks*. John Wiley and Sons, New York, 525—548.
- Pearce, J. A., 1996. Sources and Setting of Granitic Rocks. *Episodes*, 19(4): 120—125.
- Peccerillo, A., Taylor, S. R., 1976. Geochemistry of Eocene Calc-Alkaline Volcanic Rocks from the Kastamonu Area, Northern Turkey. *Contributions to Mineralogy and Petrology*, 58(1): 63—81. <https://doi.org/10.1007/bf00384745>
- Peccerillo, A., 2003. Plio-Quaternary Magmatism in Italy. *Episodes*, 26: 222—226.
- Qu, X. M., Xin, H. B., Du, D. D., et al., 2012. Ages of Post-Collisional A-Type Granite and Constraints on the Closure of the Oceanic Basin in the Middle Segment of the Bangonghu-Nujiang Suture, the Tibetan Plateau. *Geochimica*, 41(1): 1—14 (in Chinese with English abstract).
- Rapp, R. P., 1997. Heterogenous Source Regions for Archean Granitoids: Experimental and Geochemical Evidence. *Oxford Monographs on Geology and Geophysics*, 35: 267—279.
- Rickwood, P. C., 1989. Boundary Lines within Petrologic Diagrams which Use Oxides of Major and Minor Elements. *Lithos*, 22(4): 247—263. [https://doi.org/10.1016/0024-4937\(89\)90028-5](https://doi.org/10.1016/0024-4937(89)90028-5)
- Roberts, M. P., Clemens, J. D., 1993. Origin of High-Potassium, Talc-Alkaline, I-Type Granitoids. *Geology*, 21(9): 825. [https://doi.org/10.1130/0091-7613\(1993\)021<0825:oohtpa>2.3.co;2](https://doi.org/10.1130/0091-7613(1993)021<0825:oohtpa>2.3.co;2)
- Rudnick, R. L., Gao, S., 2003. Composition of the Continental Crust. *Treatise on Geochemistry*, 3: 1—64. <https://doi.org/10.1016/b0-08-043751-6/03016-4>
- Salter, V. J. M., Stracke, A., 2004. Composition of the Depleted Mantle. *Geochemistry, Geophysics, Geosystems*, 5(5): 1—27. <https://doi.org/10.1029/2003gc000597>
- Scherer, E., Munker, C., Mezger, K., 2001. Calibration of the Lutetium-Hafnium Clock. *Science*, 293(5530): 683—687. <https://doi.org/10.1126/science.1061372>
- Searle, M. P., Windley, B. F., Coward, M. P., et al., 1987. The Closing of Tethys and the Tectonics of the Himalaya. *Geological Society of America Bulletin*, 98(6): 678—701. [https://doi.org/10.1130/0016-7606\(1987\)98<678:tcotat>2.0.co;2](https://doi.org/10.1130/0016-7606(1987)98<678:tcotat>2.0.co;2)
- Sengör, A. M. C., Altın, D., Çin, A., et al., 1988. Origin and Assembly of the Tethyside Orogenic Collage at the Expense of Gondwana Land. *Geological Society, London, Special Publications*, 37(1): 119—181. <https://doi.org/10.1144/gsl.sp.1988.037.01.09>
- Shi, R. D., 2007. The Age for SSZ Ophiolite: A Restriction about Bangong Lake-Nujiang Developing. *Chinese Science*

- Bulletin*, 52(2): 223–227 (in Chinese).
- Shinjo, R., Kato, Y., 2000. Geochemical Constraints on the Origin of Bimodal Magmatism at the Okinawa Trough, an Incipient Back-Arc Basin. *Lithos*, 54 (3–4): 117–137. [https://doi.org/10.1016/s0024-4937\(00\)00034-7](https://doi.org/10.1016/s0024-4937(00)00034-7)
- Sisson, T. W., 1994. Hornblende-Melt Trace-Element Partitioning Measured by Ion Microprobe. *Chemical Geology*, 117 (1–4): 331–344. [https://doi.org/10.1016/0009-2541\(94\)90135-x](https://doi.org/10.1016/0009-2541(94)90135-x)
- Sui, Q. L., Wang, Q., Zhu, D. C., et al., 2013. Compositional Diversity of ca. 110 Ma Magmatism in the Northern Lhasa Terrane, Tibet: Implications for the Magmatic Origin and Crustal Growth in a Continent-Continent Collision Zone. *Lithos*, 168–169: 144–159. <https://doi.org/10.1016/j.lithos.2013.01.012>
- Sun, S. S., McDonough, W. F., 1989. Chemical and Isotopic Systematics of Oceanic Basalts; Implications for Mantle Composition and Processes. *Geological Society, London, Special Publications*, 42 (1): 313–345. <https://doi.org/10.1144/gsl.sp.1989.042.01.19>
- Sun, W. D., Bennett, V. C., Kamenetsky, V. S., 2004. The Mechanism of Re Enrichment in Arc Magmas; Evidence from Lau Basin Basaltic Glasses and Primitive Melt Inclusions. *Earth and Planetary Science Letters*, 222(1): 101–114. <https://doi.org/10.1016/j.epsl.2004.02.011>
- Sun, S. J., Zhang, L. P., Ding, X., et al., 2015. Zircon U-Pb Ages, Hf Isotopes and Geochemical Characteristics of Volcanic Rocks in Nagqu Area, Tibet and Their Petrogenesis. *Acta Petrologica Sinica*, 31 (7): 2063–2077 (in Chinese with English abstract).
- Taylor, S. R., McLennan, S. M., 1995. The Geochemical Evolution of the Continental Crust. *Reviews of Geophysics*, 33(2): 241–265. <https://doi.org/10.1029/95rg00262>
- Tepper, J. H., Nelson, B. K., Bergantz, G. W., et al., 1993. Petrology of the Chilliwack Batholith, North Cascades, Washington; Generation of Calc-Alkaline Granitoids by Melting of Mafic Lower Crust with Variable Water Fugacity. *Contributions to Mineralogy and Petrology*, 113 (3): 333–351. <https://doi.org/10.1007/bf00286926>
- Turner, S., Arnaud, N., Liu, J., et al., 1996. Post-Collision, Shoshonitic Volcanism on the Tibetan Plateau: Implications for Convective Thinning of the Lithosphere and the Source of Ocean Island Basalts. *Journal of Petrology*, 37(1): 45–71. <https://doi.org/10.1093/petrology/37.1.45>
- Wang, B. D., Wang, L. Q., Chung, S. L., et al., 2016. Evolution of the Bangong-Nujiang Tethyan Ocean; Insights from the Geochronology and Geochemistry of Mafic Rocks within Ophiolites. *Lithos*, 245: 18–33. <https://doi.org/10.1016/j.lithos.2015.07.016>
- Wang, Q., Zhu, D. C., Zhao, Z. D., et al., 2014. Origin of the ca. 90 Ma Magnesia-Rich Volcanic Rocks in SE Nyima, Central Tibet: Products of Lithospheric Delamination beneath the Lhasa-Qiangtang Collision Zone. *Lithos*, 198–199: 24–37. <https://doi.org/10.1016/j.lithos.2014.03.019>
- Wang, J. P., Liu, Y. M., Li, Q. S., et al., 2002. Stratigraphic Division and Geological Significance of the Jurassic Cover Sediments in the Eastern Sector of the Bangong Lake-Dêngqên Ophiolite Belt in Tibet. *Geological Bulletin of China*, 21 (7): 405–410 (in Chinese with English abstract).
- Wang, J. P., Zhao, Y. Y., Cui, Y. B., et al., 2012. LA-ICP-MS Zircon U-Pb Dating of Important Skarn Type Iron (Copper) Poly-metallic Deposits in Baingoin County of Tibet and Geochemical Characteristics of Granites. *Geological Bulletin of China*, 31(9): 1435–1450 (in Chinese with English abstract).
- Wang, Y., Zhang, Q., Qian, Q., 2000. Adakite; Geochemical Characteristics and Tectonic Significances. *Scientia Geologica Sinica*, 35(2): 251–256 (in Chinese with English abstract).
- White, W. M., Patchett, J., 1984. Hf-Nd-Sr Isotopes and Incompatible Element Abundances in Island Arcs; Implications for Magma Origins and Crust-Mantle Evolution. *Earth and Planetary Science Letters*, 67(2): 167–185. [https://doi.org/10.1016/0012-821x\(84\)90112-2](https://doi.org/10.1016/0012-821x(84)90112-2)
- Wilson, M., 1993. Magmatism and the Geodynamics of Basin Formation. *Sedimentary Geology*, 86 (1–2): 5–29. [https://doi.org/10.1016/0037-0738\(93\)90131-n](https://doi.org/10.1016/0037-0738(93)90131-n)
- Wu, F. Y., Jahn, B. M., Wilde, S. A., et al., 2003a. Highly Fractionated I-Type Granites in NE China (I): Geochronology and Petrogenesis. *Lithos*, 66 (3–4): 241–273. [https://doi.org/10.1016/s0024-4937\(02\)00222-0](https://doi.org/10.1016/s0024-4937(02)00222-0)
- Wu, F. Y., Jahn, B. M., Wilde, S. A., et al., 2003b. Highly Fractionated I-Type Granites in NE China (II): Isotopic Geochemistry and Implications for Crustal Growth in the Phanerozoic. *Lithos*, 67 (3–4): 191–204. [https://doi.org/10.1016/s0024-4937\(03\)00015-x](https://doi.org/10.1016/s0024-4937(03)00015-x)
- Wu, H., Li C., Hu, P. Y., et al., 2013. The Discovery of Qushenla Volcanic Rocks in Tasepule Area of Nyima County, Tibet, and Its Geological Significance. *Geological Bulletin of China*, 32(7): 1014–1026 (in Chinese with English abstract).
- Wu, Y., Ma, X. X., Zhang, Z. P., et al., 2016. Geochemical Features of the Nyainqentanglha Group in the Western Lhasa Terrane, Western Tibet and Their Tectonic Significance. *Acta Geologica Sinica*, 90 (11): 3081–3098 (in Chinese with English abstract).
- Wu, Y. B., Zheng, Y. F., 2004. The Research of Zircon and Its

- Restriction on the Age of U-Pb Dating, *Chinese Science Bulletin*, 49(16):1589—1604 (in Chinese).
- Xu, J.F., Wang, Q., Yu, X.Y., 2000. Geochemistry of High-Mg Andesites and Adakitic Andesite from the Sanchazi Block of the Mian-Lue Ophiolitic Melange in the Qinling Mountains, Central China; Evidence of Partial Melting of the Subducted Paleo-Tethyan Crust. *Geochemical Journal*, 34(5):359—377. <https://doi.org/10.2343/geochemj.34.359>
- Xu, R. H., Schärer, U., Allègre, C. J., 1985. Magmatism and Metamorphism in the Lhasa Block (Tibet): A Geochronological Study. *The Journal of Geology*, 93(1):41—57. <https://doi.org/10.1086/628918>
- Xu, W., Li, C., Xu, M. J., et al., 2015. Petrology, Geochemistry, and Geochronology of Boninitic Dikes from the Kangqiong Ophiolite; Implications for the Early Cretaceous Evolution of Bangong-Nujiang Neo-Tethys Ocean in Tibet. *International Geology Review*, 57(16):2028—2043. <https://doi.org/10.1080/00206814.2015.1050464>
- Xu, Z. Q., 2007. The Orogeny Plateau—The Terranes Assembly, Collision Orogenesis and Uplift Mechanism for the Tibet. Geological Publishing House, Beijing (in Chinese).
- Xu, Z. Q., Yang, J. S., Li, H. B., et al., 2011. On the Tectonics of the India-Asia Collision. *Acta Geologica Sinica*, 85(1):1—33 (in Chinese with English abstract).
- Yang, J. S., Xu, Z. Q., Li, Z. L., et al., 2009. Discovery of an Eclogite Belt in the Lhasa Block, Tibet; A New Border for Paleo-Tethys? *Journal of Asian Earth Sciences*, 34(1):76—89. <https://doi.org/10.1016/j.jseas.2008.04.001>
- Yang, T. N., Zhang, H. R., Liu, Y. X., et al., 2011. Permo-Triassic Arc Magmatism in Central Tibet; Evidence from Zircon U-Pb Geochronology, Hf Isotopes, Rare Earth Elements, and Bulk Geochemistry. *Chemical Geology*, 284(3—4):270—282. <https://doi.org/10.1016/j.chemgeo.2011.03.006>
- Yin, A., 2010. Cenozoic Tectonic Evolution of Asia; A Preliminary Synthesis. *Tectonophysics*, 488(1—4):293—325. <https://doi.org/10.1016/j.tecto.2009.06.002>
- Yin, A., Harrison, T. M., 2000. Geologic Evolution of the Himalayan-Tibetan Orogen. *Annual Review of Earth and Planetary Sciences*, 28(1):211—280. <https://doi.org/10.1146/annurev.earth.28.1.211>
- Yu, G. M., Wang, C. S., 1990. Sedimentary Geology of Tibet. Geological Publishing House, Beijing (in Chinese with English abstract).
- Zhai, Q. G., Jahn, B. M., Zhang, R. Y., et al., 2011. Triassic Subduction of the Paleo-Tethys in Northern Tibet, China; Evidence from the Geochemical and Isotopic Characteristics of Eclogites and Blueschists of the Qiangtang Block. *Journal of Asian Earth Sciences*, 42(6):1356—1370. <https://doi.org/10.1016/j.jseas.2011.07.023>
- Zhang, K. J., Xia, B. D., Wang, G. M., et al., 2004. Early Cretaceous Stratigraphy, Depositional Environments, Sandstone Provenance, and Tectonic Setting of Central Tibet, Western China. *Geological Society of America Bulletin*, 116(9):1202—1222. <https://doi.org/10.1130/b25388.1>
- Zhang, K. J., Zhang, Y. X., Tang, X. C., et al., 2012. Late Mesozoic Tectonic Evolution and Growth of the Tibetan Plateau Prior to the Indo-Asian Collision. *Earth-Science Reviews*, 114(3—4):236—249. <https://doi.org/10.1016/j.earscirev.2012.06.001>
- Zhang, L., 2015. Geochronology and Geochemistry of the Yongzhu Granitoids in Middle-North Gangdese, Tibet (Dissertation). Jilin University, Changchun, 1—84 (in Chinese with English abstract).
- Zhang, L. L., Zhu, D. C., Zhao, Z. D., et al., 2010. Petrogenesis of Magmatism in the Baerda Region of Northern Gangdese, Tibet; Constraints from Geochemistry, Geochronology and Sr-Nd-Hf Isotopes. *Acta Petrologica Sinica*, 26(6):1871—1888 (in Chinese with English abstract).
- Zhang, Q., Wang, Y., Liu, W., et al., 2002. Adakite: Its Characteristics and Implications. *Geologica Bulletin of China*, 21(7):431—435 (in Chinese with English abstract).
- Zhang, Z., Song, J. L., Tang, J. X., et al., 2017. Petrogenesis, Diagenesis and Mineralization Ages of Galale Cu-Au Deposit, Tibet; Zircon U-Pb Age, Hf Isotopic Composition and Molybdenite Re-Os Dating. *Earth Science*, 42(6):862—880 (in Chinese with English abstract).
- Zheng, Y. Y., Ci, Q., Wu, S., et al., 2017. The Discovery and Significance of Rongga Porphyry Mo Deposit in the Bangong-Nujiang Metallogenic Belt, Tibet. *Earth Science*, 42(9):1441—1453 (in Chinese with English abstract).
- Zhu, D. C., Li, S. M., Cawood, P. A., et al., 2016. Assembly of the Lhasa and Qiangtang Terranes in Central Tibet by Divergent Double Subduction. *Lithos*, 245:7—17. <https://doi.org/10.1016/j.lithos.2015.06.023>
- Zhu, D. C., Mo, X. X., Niu, Y. L., et al., 2009. Geochemical Investigation of Early Cretaceous Igneous Rocks along an East-West Traverse throughout the Central Lhasa Terrane, Tibet. *Chemical Geology*, 268(3—4):298—312. <https://doi.org/10.1016/j.chemgeo.2009.09.008>
- Zhu, D. C., Zhao, Z. D., Niu, Y. L., et al., 2011. The Lhasa Terrane: Record of a Microcontinent and Its Histories of Drift and Growth. *Earth and Planetary Science Letters*, 301(1—2):241—255. <https://doi.org/10.1016/j.epsl.2010.11.005>
- Zhu, D. C., Zhao, Z. D., Niu, Y. L., et al., 2013. The Origin and

- Pre-Cenozoic Evolution of the Tibetan Plateau. *Gondwana Research*, 23(4): 1429–1454. <https://doi.org/10.1016/j.gr.2012.02.002>
- Zhu, D.C., Pan, G.T., Wang, L.Q., et al., 2008. Tempo-Spatial Variations of Mesozoic Magmatic Rocks in the Gangdise Belt, Tibet, China, with a Discussion of Geodynamic Setting-Related Issues. *Geological Bulletin of China*, 27(9): 1535–1550 (in Chinese with English abstract).
- Zhu, D.C., Pan, G.T., Mo, X.X., et al., 2006a. Late Jurassic–Early Cretaceous Geodynamic Setting in Middle–Northern Gangdise: New Insights from Volcanic Rocks. *Acta Petrologica Sinica*, 22(3): 534–546 (in Chinese with English abstract).
- Zhu, D.C., Pan, G.T., Mo, X.X., et al., 2006b. Identification for the Mesozoic OIB-Type Basalts in Central Qiangtang–Tibetan Plateau: Geochronology, Geochemistry and Their Tectonic Setting. *Acta Geologica Sinica*, 80(9): 1312–1328 (in Chinese with English abstract).
- Zhu, Z.Y., Wang, T.W., Li, C., 2004. Metamorphic Characteristics of Nyainqentanglha Group in Jielangya Area of Bange, Tibet. *Global Geology*, 23(2): 128–133 (in Chinese with English abstract).
- Zorpi, M.J., Coulon, C., Orsini, J.B., 1991. Hybridization between Felsic and Mafic Magmas in Calc-Alkaline Granitoids—A Case Study in Northern Sardinia, Italy. *Chemical Geology*, 92(1–3): 45–86. [https://doi.org/10.1016/0009-2541\(91\)90049-w](https://doi.org/10.1016/0009-2541(91)90049-w)
- ### 附中文参考文献
- 陈国荣, 刘鸿飞, 蒋光武, 等, 2004. 西藏班公湖—怒江结合带中段沙木罗组的发现. *地质通报*, 23(2): 193–194.
- 陈越, 朱弟成, 赵志丹, 等, 2010. 西藏北冈底斯巴木错安山岩的年代学、地球化学及岩石成因. *岩石学报*, 26(7): 2193–2206.
- 陈玉禄, 张宽忠, 杨志民, 等, 2006. 青藏高原班公湖—怒江结合带中段那曲县觉翁地区发现完整的蛇绿岩剖面. *地质通报*, 25(6): 694–699.
- 邓晋福, 肖庆辉, 苏尚国, 等, 2007. 火成岩组合与构造环境: 讨论. *高校地质学报*, 13(3): 392–402.
- 定立, 赵元艺, 杨永强, 等, 2012. 西藏班戈县多巴区矽卡岩型铁多金属矿床含矿花岗岩 LA-ICP-MS 锆石 U-Pb 定年、地球化学及意义. *岩石矿物学杂志*, 31(4): 479–496.
- 丁帅, 唐菊兴, 郑文宝, 等, 2017. 西藏拿若斑岩型铜(金)矿含矿岩体年代学、地球化学及地质意义. *地球科学*, 42(1): 1–23.
- 樊树权, 史仁灯, 丁林, 等, 2010. 西藏改则蛇绿岩中斜长花岗岩地球化学特征、锆石 U-Pb 年龄及构造意义. *岩石矿物学杂志*, 29(5): 467–478.
- 高顺宝, 郑有业, 王进寿, 等, 2011a. 西藏班戈地区侵入岩年代学和地球化学: 对班公湖—怒江洋盆演化时限的制约. *岩石学报*, 27(7): 1973–1982.
- 高顺宝, 郑有业, 谢名臣, 等, 2011b. 西藏班戈地区雪如岩体的形成环境及成矿意义. *地球科学*, 36(4): 729–739.
- 高永丰, 侯增谦, 魏瑞华, 2003. 冈底斯晚第三纪斑岩的岩石学、地球化学及其地球动力学意义. *岩石学报*, 19(3): 418–428.
- 耿全如, 毛晓长, 张璋, 等, 2015. 班公湖—怒江成矿带中、西段岩浆弧新认识及其对找矿的启示. *中国地质调查*, 2(2): 1–11.
- 耿全如, 潘桂棠, 王立全, 等, 2011. 班公湖—怒江带、羌塘地块特提斯演化与成矿地质背景. *地质通报*, 30(8): 1261–1274.
- 关俊雷, 耿全如, 王国芝, 等, 2014. 北冈底斯带日土县—拉梅拉山口花岗岩体的岩石地球化学特征、锆石 U-Pb 测年及 Hf 同位素组成. *岩石学报*, 30(06): 1666–1684.
- 侯可军, 李延河, 邹天人, 等, 2007. LA-MC-ICP-MS 锆石 Hf 同位素的分析方法及地质应用. *岩石学报*, 23(10): 2595–2604.
- 胡隼, 万永文, 陶专, 等, 2014. 班公湖—怒江缝合带西段特提斯洋盆南向俯冲的地球化学和年代学证据. *成都理工大学学报(自然科学版)*, 41(4): 505–515.
- 黄瀚霄, 李光明, 董随亮, 等, 2012. 西藏班戈地区青龙花岗闪长岩 SHRIMP 锆石 U-Pb 年龄及其地球化学特征. *地质通报*, 31(6): 852–859.
- 黄玉, 朱弟成, 赵志丹, 等, 2012. 西藏北部拉萨地块那曲地区约 113 Ma 安山岩岩石成因与意义. *岩石学报*, 28(5): 1603–1614.
- 康磊, 校培喜, 高晓峰, 等, 2012. 青藏高原西北缘红其拉甫岩体的岩石成因、时代及其构造意义. *地质学报*, 86(7): 1063–1076.
- 康志强, 许继峰, 王保弟, 等, 2009. 拉萨地块北部白垩纪多尼组火山岩的地球化学: 形成的构造环境. *地球科学*, 34(1): 89–104.
- 李才, 翟刚毅, 王立全, 等, 2009. 认识青藏高原的重要窗口——羌塘地区近年来研究进展评述(代序). *地质通报*, 28(9): 1169–1177.
- 李小波, 王保弟, 刘函, 等, 2015. 西藏达如错地区晚侏罗世高镁安山岩—班公湖—怒江洋壳俯冲消减的证据. *地质通报*, 34(2–3): 251–261.
- 莫宣学, 董国臣, 赵志丹, 等, 2005. 西藏冈底斯带花岗岩的时空分布特征及地壳生长演化信息. *高校地质学报*, 11(3): 281–290.
- 莫宣学, 潘桂棠, 2006. 从特提斯到青藏高原形成: 构造—岩浆事件的约束. *地学前缘*, 13(6): 43–51.
- 莫宣学, 赵志丹, 邓晋富, 等, 2003. 印度—亚洲大陆主碰撞过

- 程的火山作用响应.地学前缘,10(3): 135-148.
- 潘桂棠,莫宣学,侯增谦,等,2006.冈底斯造山带的时空结构及演化.岩石学报,22(3): 521-533.
- 潘桂棠,朱弟成,王立全,等,2004.班公湖-怒江缝合带作为冈瓦纳大陆北界的地质地球物理证据.地学前缘,11(4): 372-382.
- 曲晓明,辛洪波,杜德道,等,2012.西藏班公湖-怒江缝合带中段碰撞后 A 型花岗岩的时代及其对洋盆闭合时间的约束.地球化学,41(1): 1-14.
- 史仁灯,2007.班公湖 SSZ 型蛇绿岩年龄对班-怒洋时的制约.科学通报,52(2): 223-227.
- 孙赛军,张丽鹏,丁兴,等,2015.西藏那曲中酸性火山岩的锆石 U-Pb 年龄、Hf 同位素和地球化学特征及岩石成因.岩石学报,31(7): 2063-2077.
- 王建平,刘彦明,李秋生,等,2002.西藏班公湖-丁青蛇绿岩带东段侏罗纪盖层沉积的地层划分.地质通报,21(7): 405-410.
- 王江朋,赵元艺,崔玉斌,等,2012.西藏班戈地区重要矽卡岩型铁(铜)多金属矿床 LA-ICP-MS 锆石 U-Pb 测年与花岗岩地球化学特征.地质通报,31(9): 1435-1450.
- 王焰,张旗,钱青,2000.埃达克岩(adakite)的地球化学特征及其构造意义.地质科学,35(2): 251-256.
- 吴浩,李才,胡培远,等,2013.西藏尼玛县塔色普勒地区去申拉组火山岩的发现及其地质意义.地质通报,32(7): 1014-1026.
- 吴勇,马绪宣,张志平,等,2016.青藏高原拉萨地块西部念青唐古拉岩群的地球化学特征及构造意义.地质学报,90(11): 3081-3098.
- 吴元保,郑永飞,2004.锆石成因矿物学研究及其对 U-Pb 年龄解释的制约.科学通报,49(16): 1589-1604.
- 许志琴,2007.造山的高原——青藏高原的地体拼合、碰撞造山及隆升机制.北京:地质出版社.
- 许志琴,杨经绥,李海兵,等,2011.印度-亚洲碰撞大地构造.地质学报,85(1): 1-33.
- 余光明,王成善,1990.西藏特提斯沉积地质.北京:地质出版社.
- 张乐,2015.西藏冈底斯中北部永珠地区花岗岩类年代学与地球化学(硕士学位论文).长春:吉林大学,1-84.
- 张亮亮,朱弟成,赵志丹,等,2010.西藏北岗底斯巴达尔地区岩浆作用的成因:地球化学、年代学及 Sr-Nd-Hf 同位素约束.岩石学报,26(6): 1871-1888.
- 张旗,王焰,刘伟,等,2002.埃达克岩的特征及其意义.地质通报,21(7): 431-435.
- 张志,宋俊龙,唐菊兴,等,2017.西藏嘎啦勒铜金矿床的成岩成矿时代与岩石成因:锆石 U-Pb 年龄、Hf 同位素组成及辉钼矿 Re-Os 定年.地球科学,42(6): 862-880.
- 郑有业,次琼,吴松,等,2017.西藏班公湖-怒江成矿带荣嘎斑岩型钼矿床的发现及意义.地球科学,42(9): 1441-1453.
- 朱弟成,潘桂棠,莫宣学,等,2006a.冈底斯中北部晚侏罗世-早白垩世地球动力学环境:火山岩约束.岩石学报,22(3): 534-546.
- 朱弟成,潘桂棠,莫宣学,等,2006b.青藏高原中部中生代 OIB 型玄武岩的识别:年代学、地球化学及其构造环境.地质学报,80(9): 1312-1328.
- 朱弟成,潘桂棠,王立全,等,2008.西藏冈底斯带中生代岩浆岩的时空分布和相关问题的讨论.地质通报,27(9): 1535-1550.
- 朱志勇,王天武,李才,2004.西藏班戈节浪垭地区念青唐古拉群变质作用特征.世界地质,23(2): 128-133.